

CHAPTER IV

RESULTS AND DISCUSSION

4.1 Adsorption Isotherm of CTAB onto Silica Hi-Sil[®]255

The adsorption isotherm of CTAB onto Hi-Sil[®]255 is shown in Figure 4.1. The isotherm clearly shows regions II, III and IV of the typical surfactant adsorption isotherm. The experimentally determined critical micelle concentration (CMC) of 900 μM was very close to the 920 μM reported by Rosen (1989). From the plateau adsorption region, the maximum adsorption was 600 μmole of CTAB per gram of silica. Regarding to the adsorption isotherm, the initial CTAB concentration which gives an equilibrium bulk concentration just below the CMC, for a ratio of one kilogram of silica per 12.5 liters solution, was 48,900 μM .

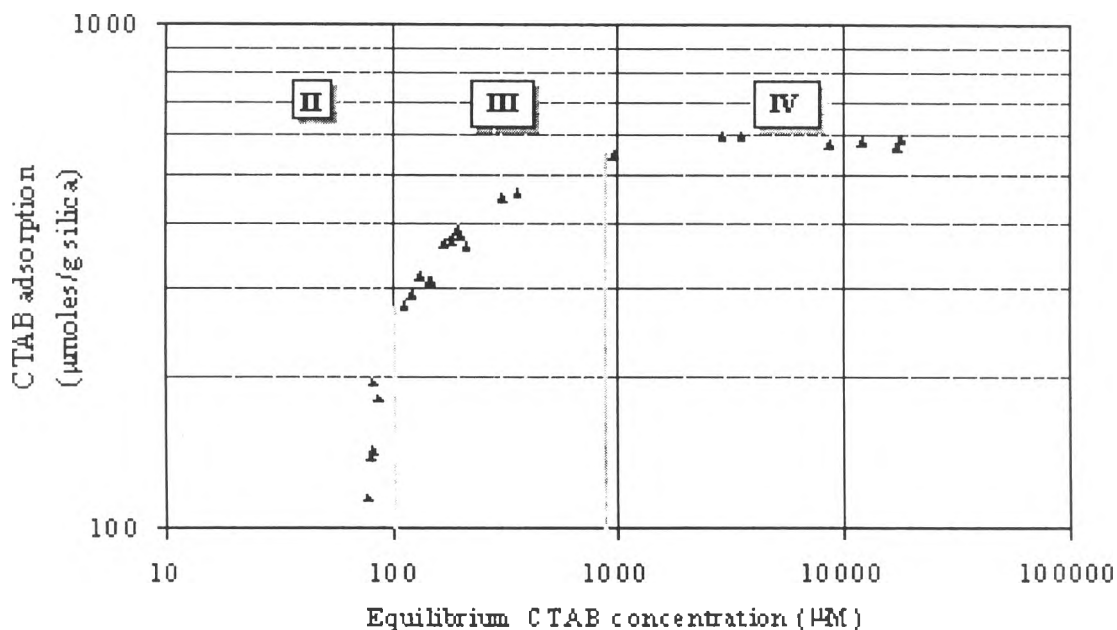


Figure 4.1 Adsorption isotherm of CTAB onto silica Hi-Sil[®]255 at pH 8 and 30°C.

Assuming monolayer adsorption and access to the entire measured BET surface area, CTAB molecules occupy 47 \AA^2 per head group in the plateau region. This value can be compared to tetradecyltrimethyl ammonium bromide ($\text{C}_{14}\text{H}_{29}\text{N}(\text{CH}_3)_3^+\text{Br}^-$) and octadecyltrimethylammonium bromide ($\text{C}_{18}\text{H}_{37}\text{N}(\text{CH}_3)_3^+\text{Br}^-$) which respectively have surface areas of 61 \AA^2 and 64 \AA^2 per molecule at a saturated water-air interface (Rosen, 1989). As CTAB would not have access into the smaller pores of the silica, the area per head group on the silica surface would be even less than the calculated 47 \AA^2 . Hence, it is strongly believed that the CTAB aggregates on the silica surface is most likely in the form of a bilayer.

4.2 Flow Pattern of Studied CSTR System

Before performing the CSTR experiment for admicellar polymerization on the silica surface, a flow pattern of the reactor was tested to ensure complete mixing. A pulse test using NaOH was performed. As shown in Figure 4.2, complete mixing can be achieved and so theoretically, the reactor is a CSTR system.

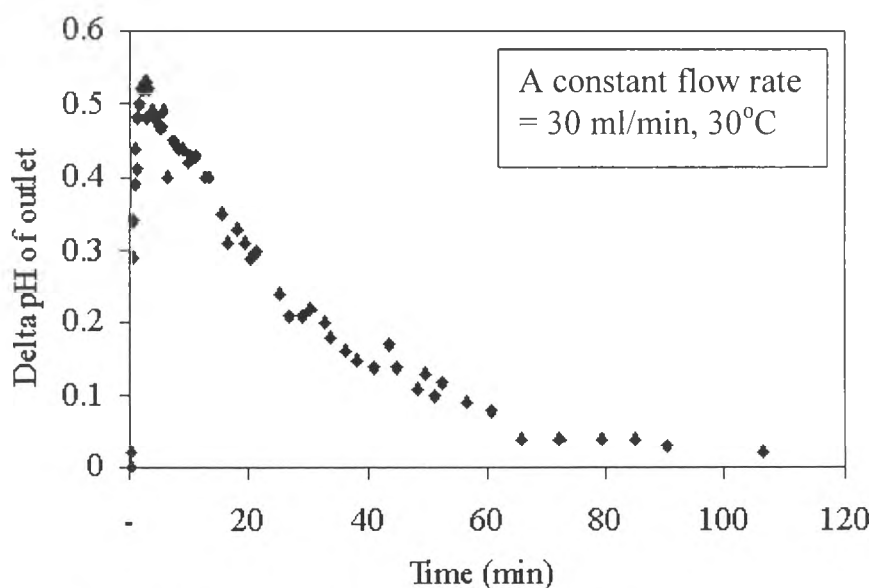


Figure 4.2 Pulse test of reactor by injection of NaOH.

4.3 Determination of Steady State Time of Studied System

To determine the time needed for the system to reach steady state, the fluid samples leaving the reactor as a function of time were analyzed for carbon contents using the Total Organic Carbon analyzer. The modification of silica with 40-g styrene-isoprene loading per kilogram of silica at 120 minutes retention time was used for this purpose. Polymerization was carried out at 70°C. The carbon content represents the amount of CTAB and styrene-isoprene monomers dissolved in the product supernatant. As seen in the figure, the TOC decreases for the first 30 min, indicating the consumption of monomers during the initiation of the polymerization process. After 30 to 40 minutes, the TOC becomes stable, indicating the steady-state operating conditions. As shown in Figure 4.3, the time to reach steady state is approximately 70 minutes which is insignificant compared to the total reaction run time of up to 13 hours. Therefore, all effluent was collected in the product tank.

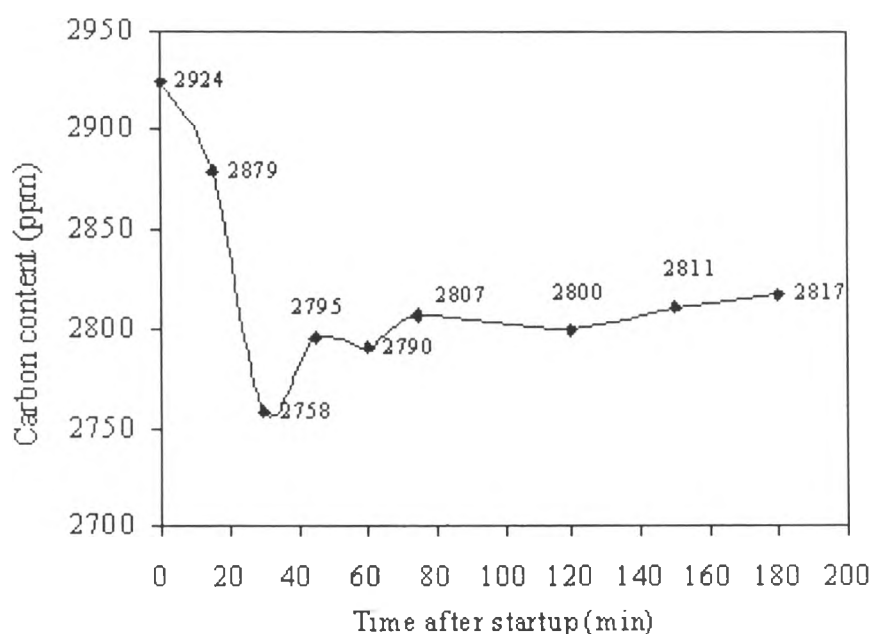


Figure 4.3 Relationship between carbon content and time after startup .

4.4 Surface Characterization of Modified Silicas

The admicellar polymerization process has been known to affect a variety of the physical characteristics of silica, including BET surface area and mean agglomerate particle size. All samples were given a designation consisting of a number indicating the amount of monomer (styrene-isoprene) loading (5, 20 and 30, in units of grams of co-monomers per kilogram of silica), and a letter representing polymerization retention time. The polymerization times of 30, 45 and 60 minutes are denoted by S, M and L, respectively. The 20 grams co-monomers with 45 minutes retention time was duplicated twice, with the sample designations of 20M1 and 20M2.

4.4.1 BET Surface Area

All modified silica samples had BET surface areas less than that of the unmodified silica, some by as much as 20% (see Figure 4.4). For each level of monomer loading, the modified silica with a 60-minute retention time had the lowest surface area, while the highest surface areas were obtained with a 45-minute reaction time. Though the reason for this is unclear, the following scenario is a possible explanation. At low monomer loadings, it is more likely that small aggregates of polymer are formed, primarily in the pores of this highly porous silica. This polymer partially blocks the pores, causing a decrease in surface area. At intermediate monomer levels, polymer forms both on the surface and in the pores, but during the washing process many of these surface aggregates are removed, exposing the silica surface. At high monomer loadings, the surface of the silica is nearly encased in polymer, forming a film that is not easily removed and which effectively blocks most nitrogen access to pores.

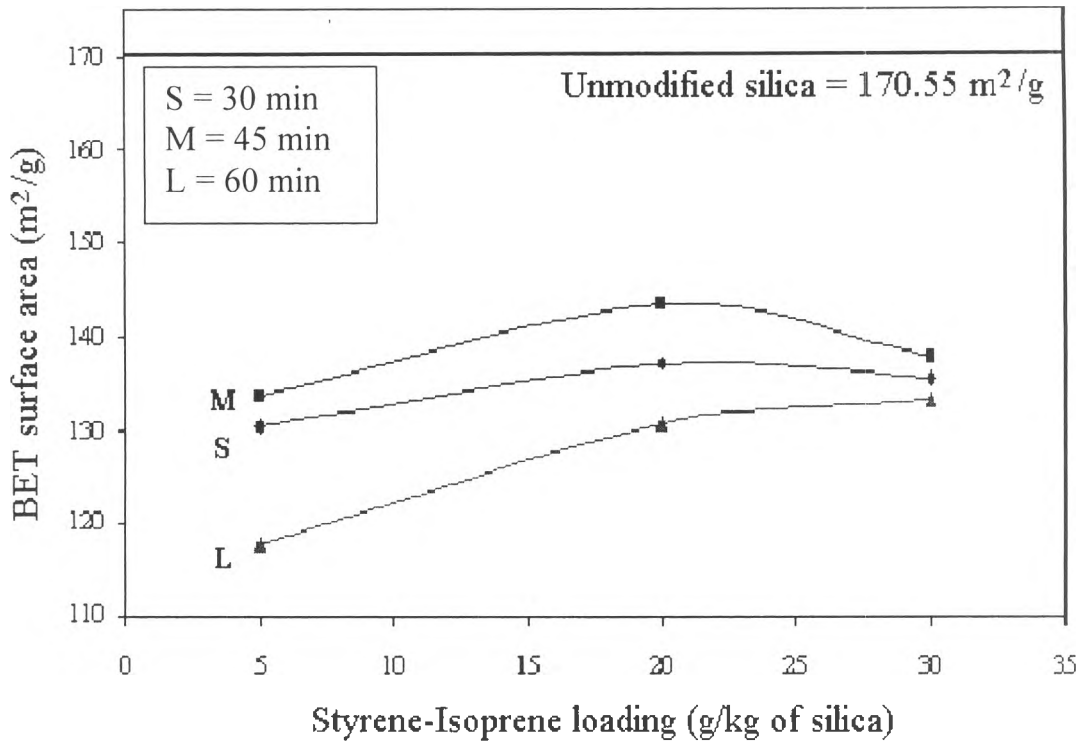


Figure 4.4 BET surface area of modified silica as a function of retention time and styrene-isoprene loading.

4.4.2 Mean Agglomerate Particle Size

Figure 4.5 shows the effect of retention time and co-monomer loading on mean agglomerate particle size. As can be seen from Figure 4.5, the mean agglomerate particle size of all modified silicas increased, some by as much as 16%. The 45-minute retention time samples consistently resulted in the highest degree of agglomeration while the 30-minute time samples had the smallest degree of agglomeration over all three levels of co-monomer loadings. It has previously been stated that the reason for an increase in aggregate size might be due to the processing of the silica, specifically, grinding it back to a powder by forcing it through a sieve (Chinpan, 1996). However, the consistent trends found in this study cast some doubt on that hypothesis. The increase in the mean agglomerate particle size may result from the development of polymer bridges between silica particles. The

observed trends may be due to changes in the distribution of monomers within the admicelle at different loadings. At low monomer feed levels, there are fewer monomers located in the exposed surface admicelles. Thus, the likelihood of particles “bonding” is small. At intermediate levels, the monomer(s) are evenly distributed, making the joining of contacting particles likely. At high loadings, the monomer may begin to phase separate within the admicelle, forming “pools” of monomer, enriching some areas, depleting others, which would again decrease the likelihood of particles joining. However, the reason for the observed behavior is not completely understood at this time.

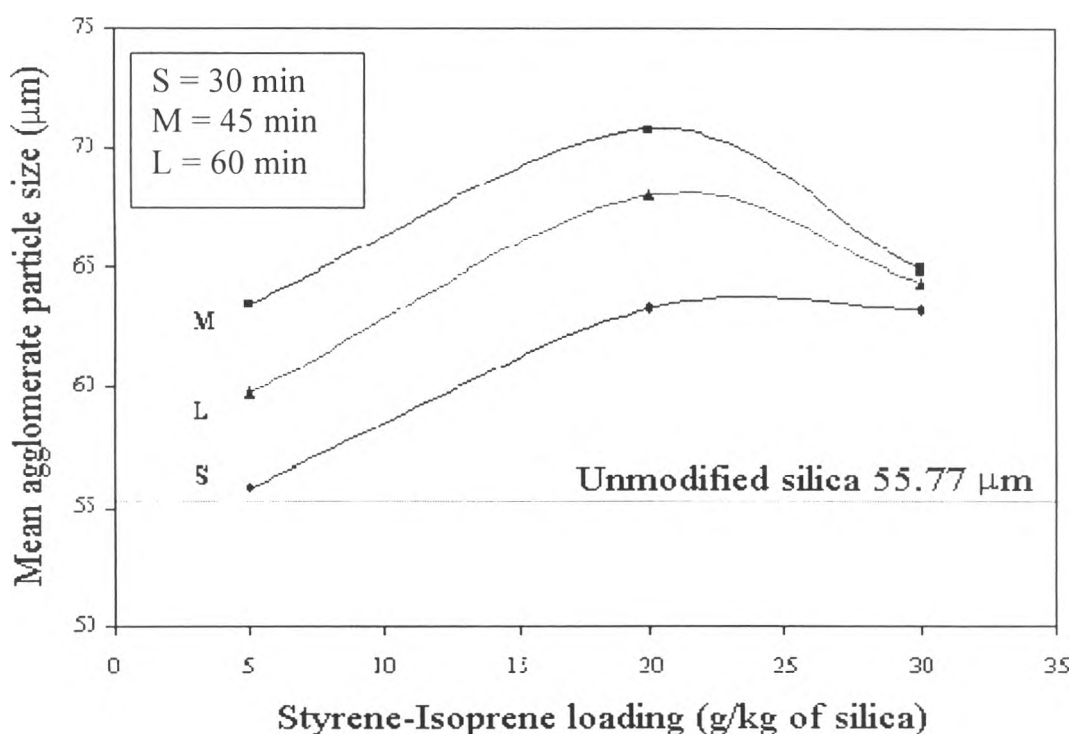


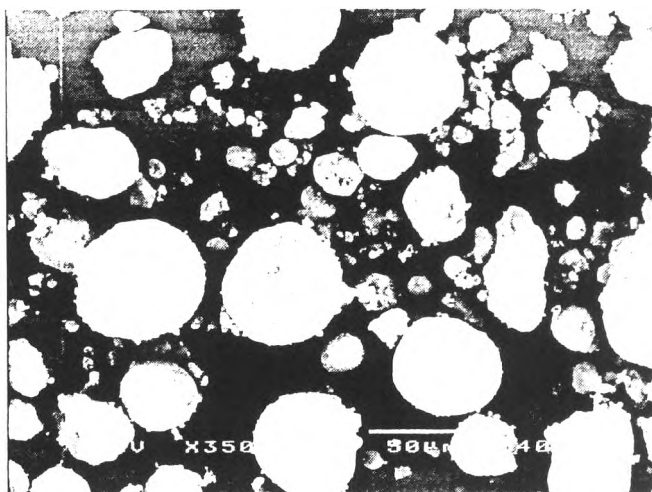
Figure 4.5 Mean agglomerate particle size of modified silicas as a function of retention time and styrene-isoprene loading.

4.4.3 Morphology of Modified Silicas

The scanning electron micrographs of unmodified silica and the various modified silicas are shown in Figures 4.6 to 4.16. Comparisons

between the unmodified and modified silica images also show that the small particles present in the unmodified silica samples disappear after modification, which may be caused by the washing process or by their “bonding” to the larger aggregates during the modification process. The micrographs clearly revealed that the particle size of silica increased with increasing the monomers loading. Interestingly, the surfaces of most modified silica samples appeared smooth as compared to the rough surface of unmodified silica. The formation of polystyrene layer on the silica surface results to the smooth appearance.

A.
at 350 X Magnification.



B.
at 2,000 X Magnification.

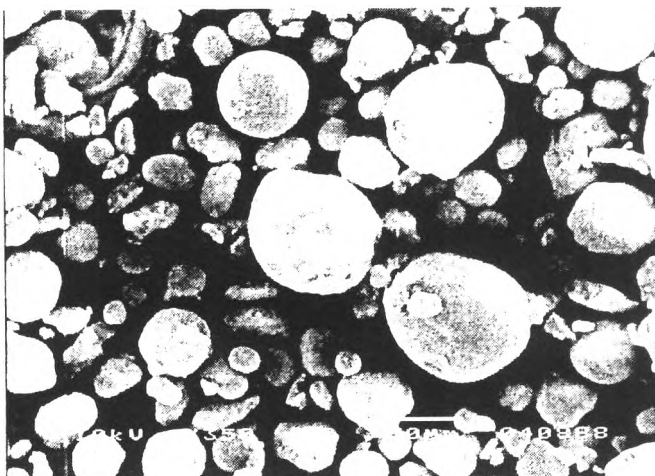


C.
at 7,500 X Magnification.



Figure 4.6 Scanning electron micrographs of unmodified silica, Hi-Sil[®]255.

A.
at 350 X Magnification.



B.
at 2,000 X Magnification.

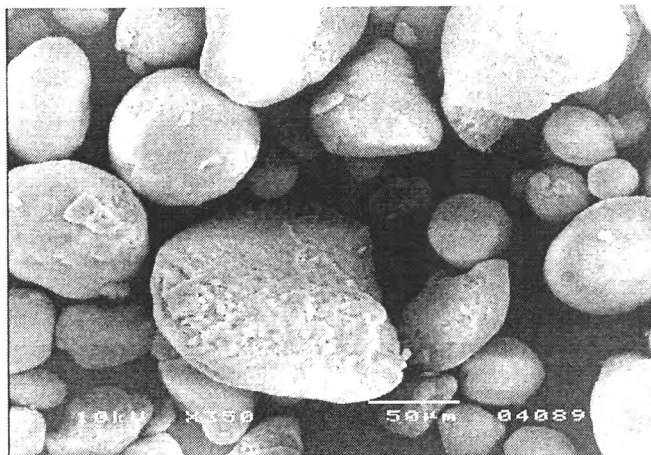


C.
at 7,500 X Magnification.



Figure 4.7 Scanning electron micrographs of modified silica, 5S.

A.
at 350 X Magnification.



B.
at 2,000 X Magnification.



C.
at 7,500 X Magnification.

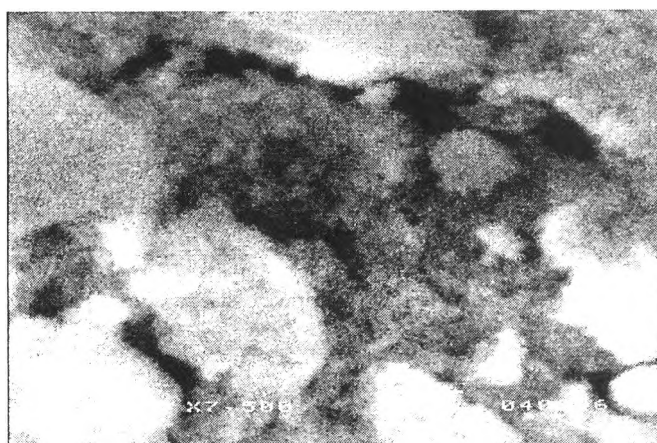
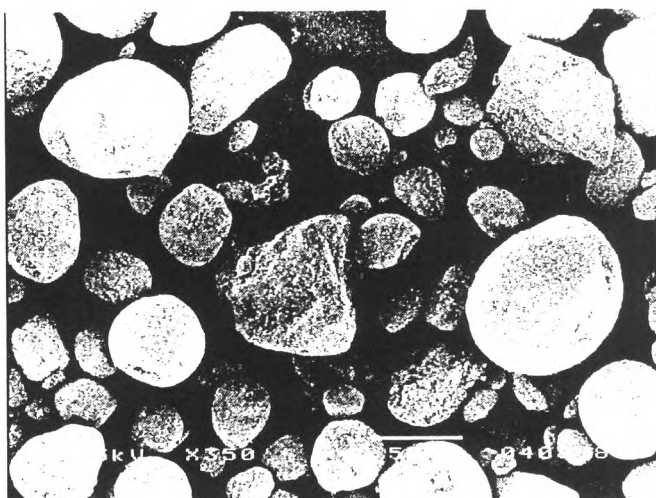
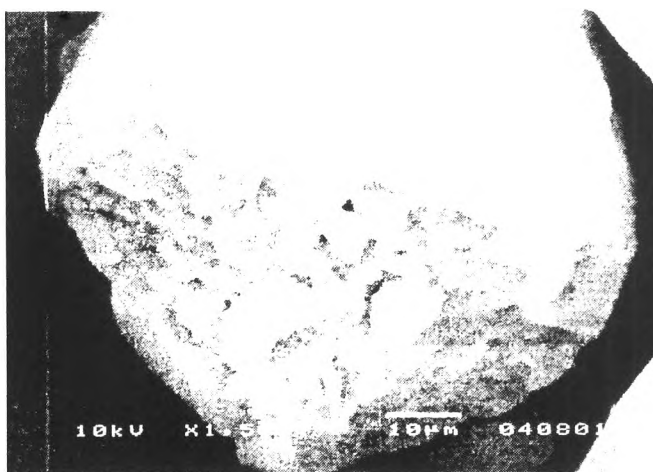


Figure 4.8 Scanning electron micrographs of modified silica, 5M.

A.
at 350 X Magnification.



B.
at 1,500 X Magnification.



C.
at 5,000 X Magnification.

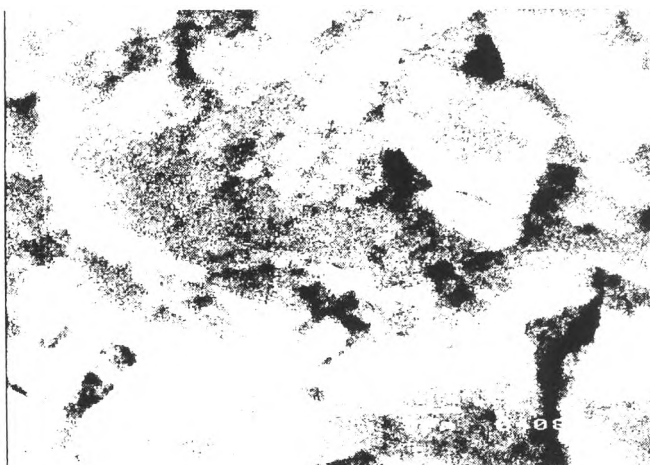
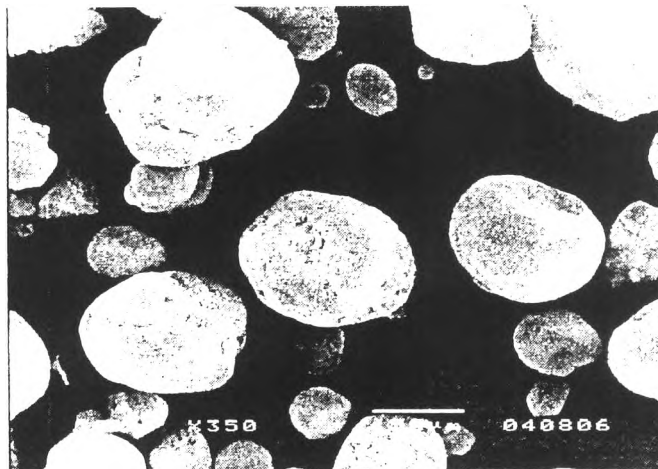
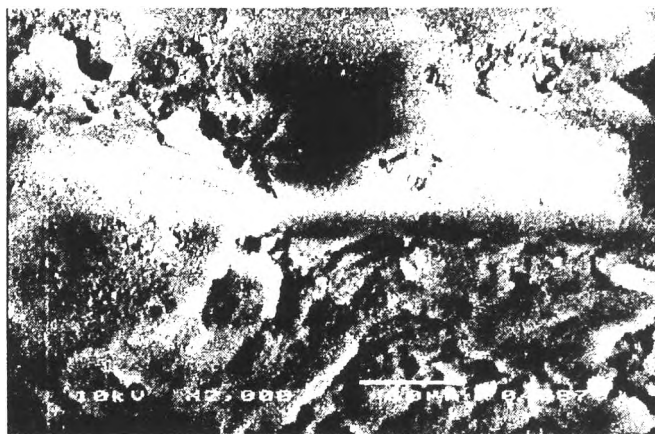


Figure 4.9 Scanning electron micrographs of modified silica, 5L,

A.
at 350 X Magnification.



B.
at 2,000 X Magnification.



C.
at 7,500 X Magnification.

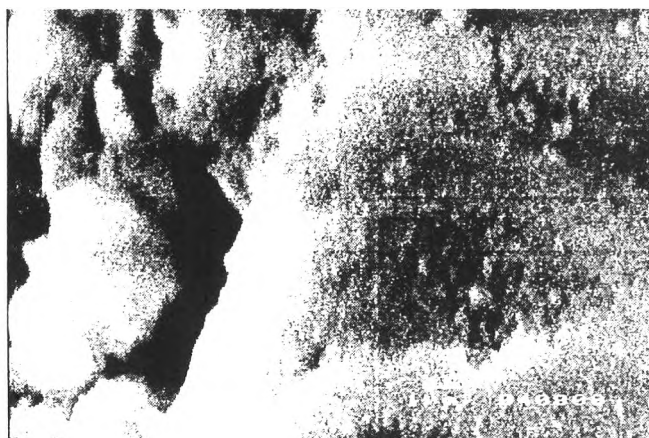
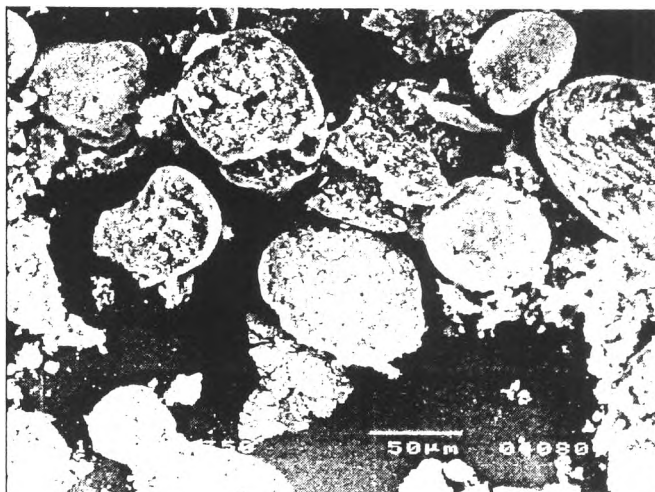
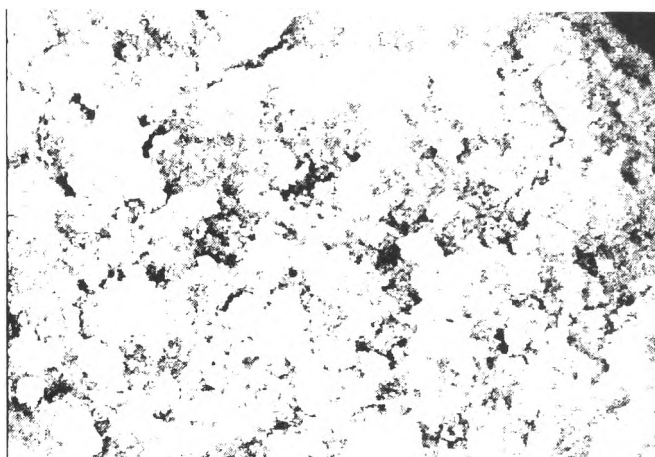


Figure 4.10 Scanning electron micrographs of modified silica, 20S.

A.
at 350 X Magnification.



B.
at 2,000 X Magnification.



C.
at 7,500 X Magnification.

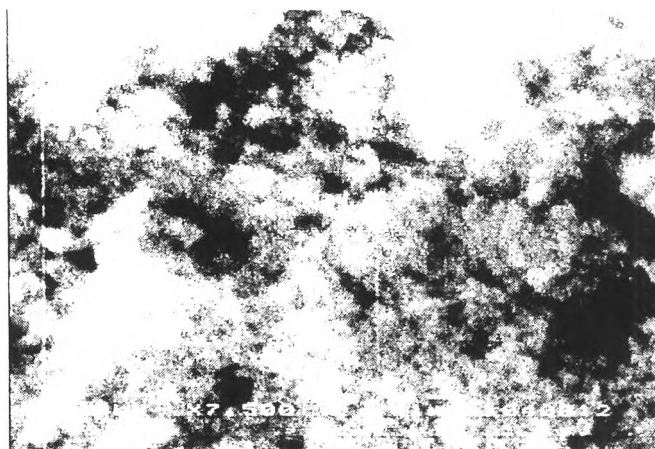
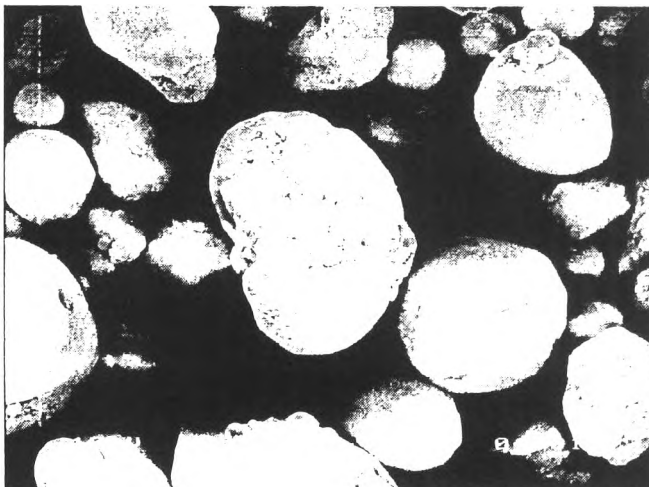


Figure 4.11 Scanning electron micrographs of modified silica, 20M1.



A.
at 350 X Magnification.



B.
at 2,000 X Magnification.

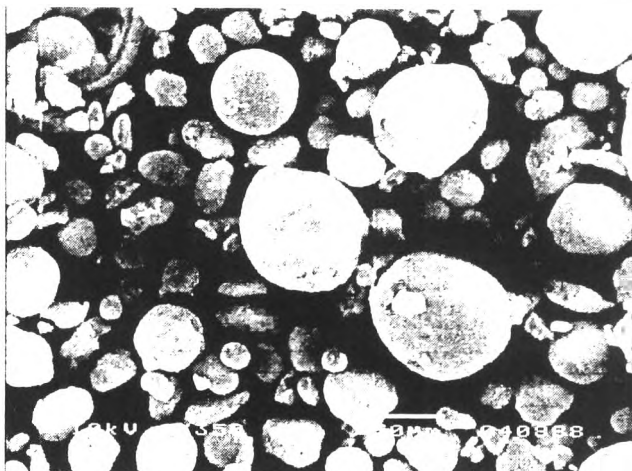


C.
at 7,500 X Magnification.



Figure 4.12 Scanning electron micrographs of modified silica, 20M2.

A.
at 350 X Magnification.



B.
at 2,000 X Magnification.

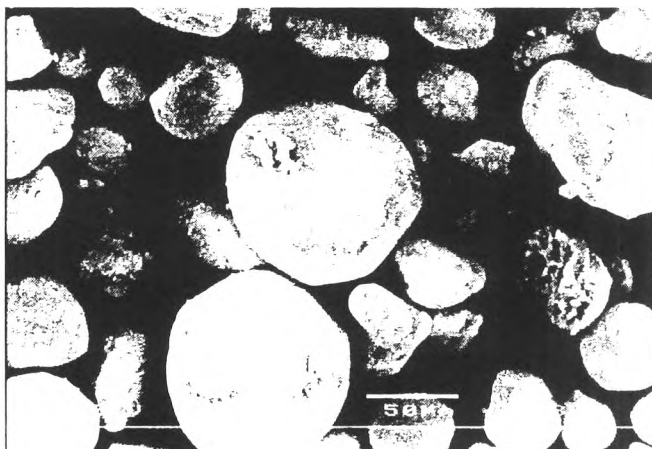


C.
at 7,500 X Magnification.



Figure 4.13 Scanning electron micrographs of modified silica, 20L.

A.
at 350 X Magnification.



B.
at 2,000 X Magnification.



C.
at 7,500 X Magnification.

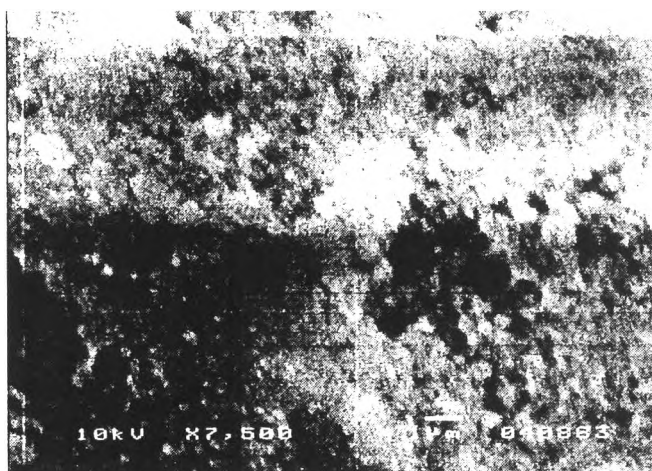
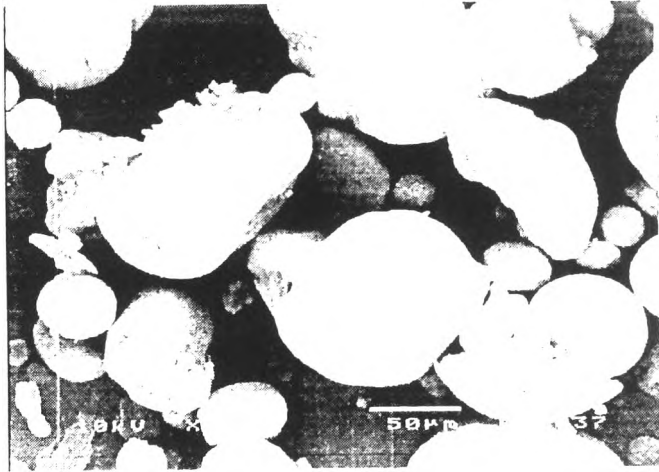


Figure 4.14 Scanning electron micrographs of modified silica, 30S.

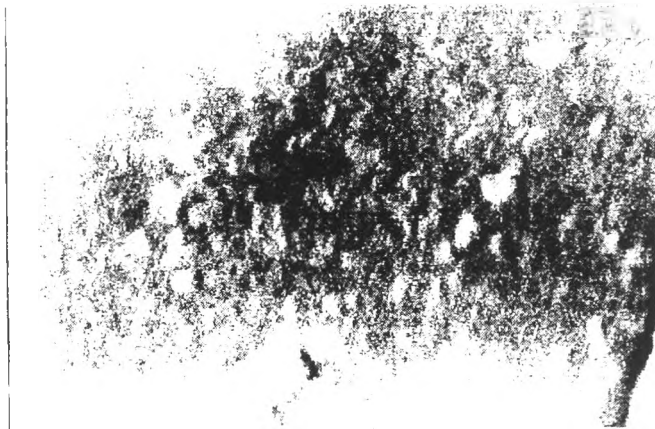
A.
at 350 X Magnification.



B.
at 2,000 X Magnification.

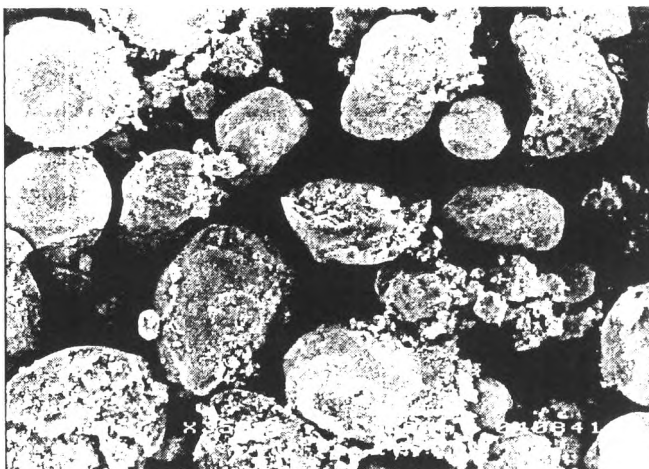


C.
at 7,500 X Magnification.

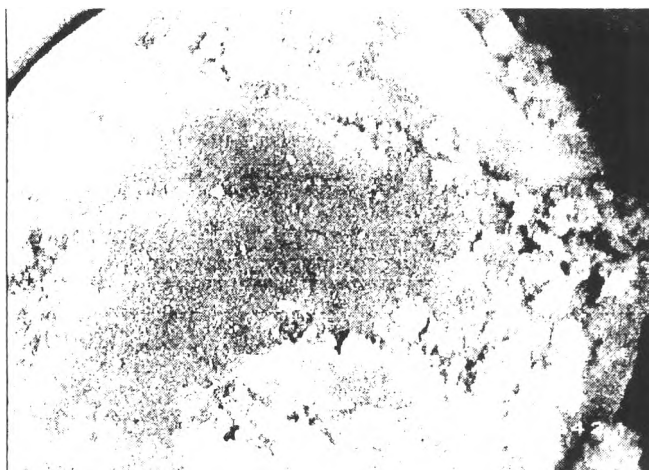


A. **Figure 4.15** Scanning electron micrographs of modified silica, 30M.

A.
at 350 X Magnification,



B.
at 2,000 X Magnification.



C.
at 7,500 X Magnification.

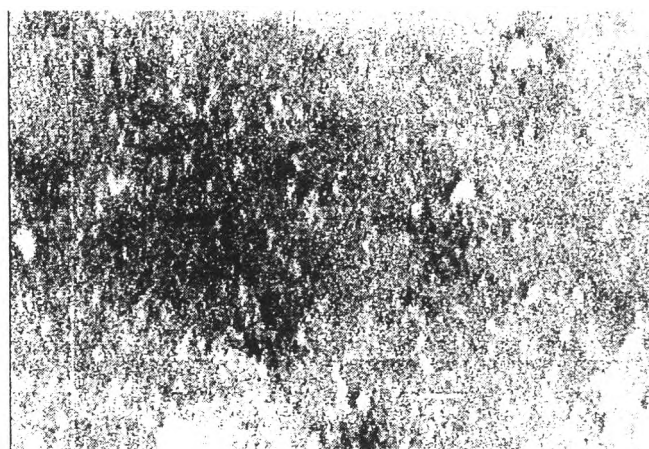


Figure 4.16 Scanning electron micrographs of modified silica, 30L.

4.4.4 Fourier Transform Infrared Spectroscopy (FT-IR) Results

Polymer from the modified silicas was extracted by refluxing with tetrahydrofuran (THF). The extracted material and the silica after the extraction were analyzed by FT-IR in order to prove the existence of poly(styrene-isoprene) on the silica surface. Figure 4.17 illustrates the FT-IR spectra of CTAB adsorbed onto silica clearly showing the characteristic peaks of CTAB. Figure 4.18 is the spectra of poly(styrene-isoprene) produced by the emulsion polymerization of the monomers in a micellar CTAB solution. The characteristic benzene ring functional group peak at a wave number of 700 cm^{-1} proves the existence of styrene while the characteristic aliphatic carbon double bond (C=C) peak at 1600 cm^{-1} proves the presence of isoprene. The spectra of all modified silicas, silica after the extraction and of the extracted materials are shown in Figures 4.19-4.28. Again, the spectra provide evidence of the existence of poly(styrene-isoprene) on the silica surface, though interference from silica and CTAB spectra nearly mask that of the polymer functional groups.

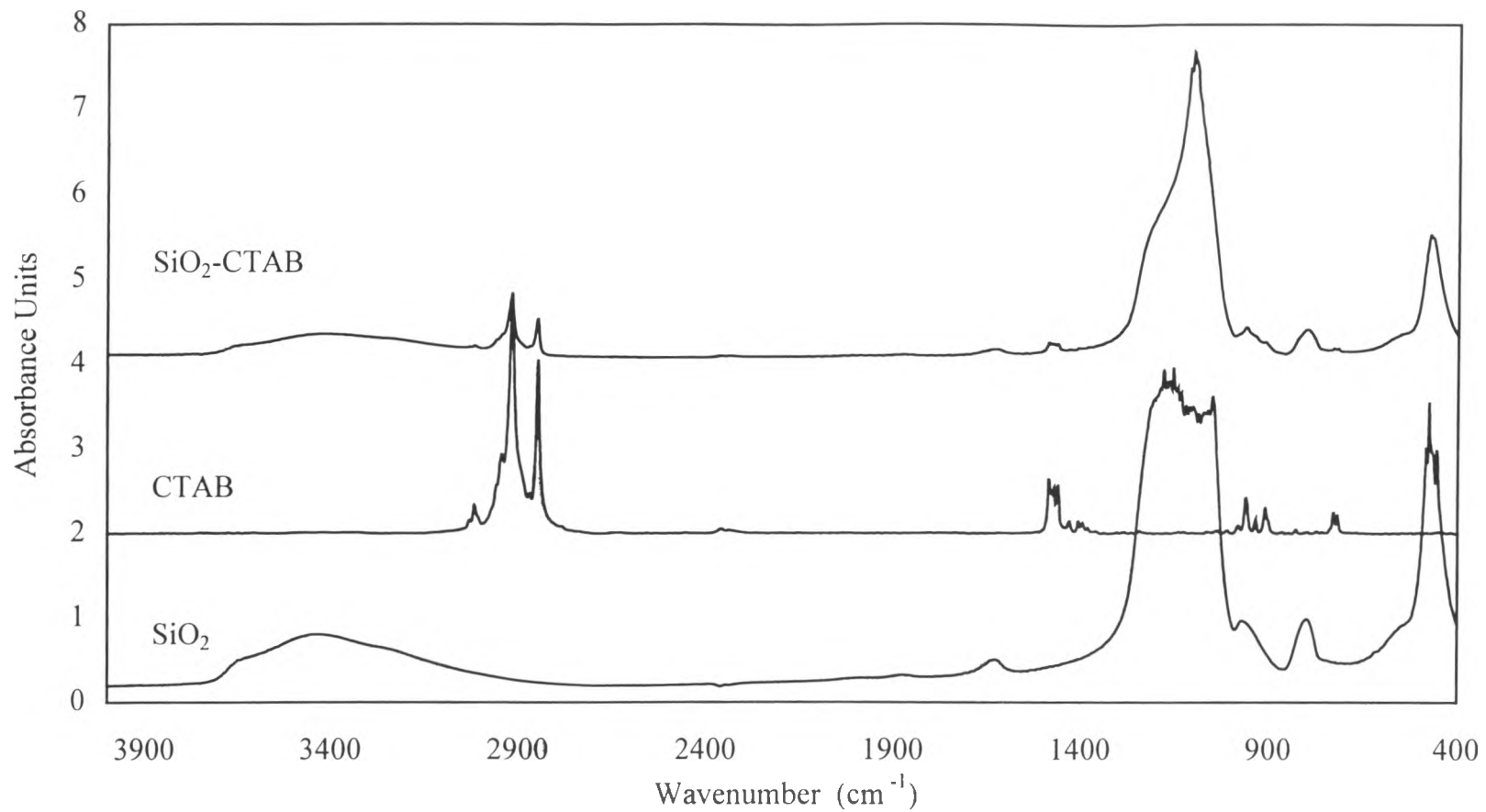


Figure 4.17 FT-IR spectra of unmodified silica (SiO₂), CTAB and unmodified silica adsorped with CTAB (SiO₂-CTAB).

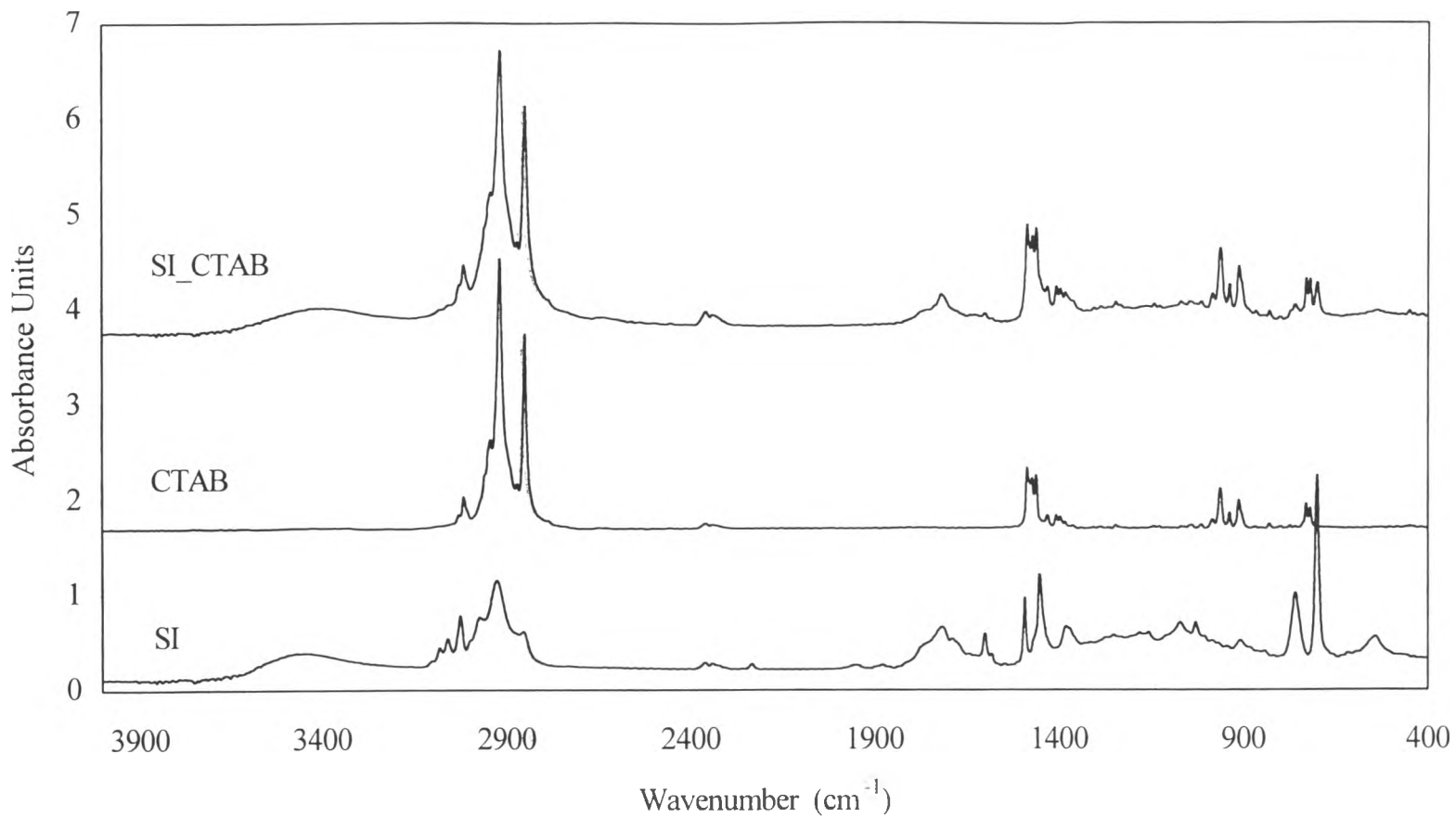


Figure 4.18 FT-IR spectra of poly(styrene-isoprene) (SI), CTAB and poly(styrene-isoprene) polymerized in CTAB solution (SI_CTAB).

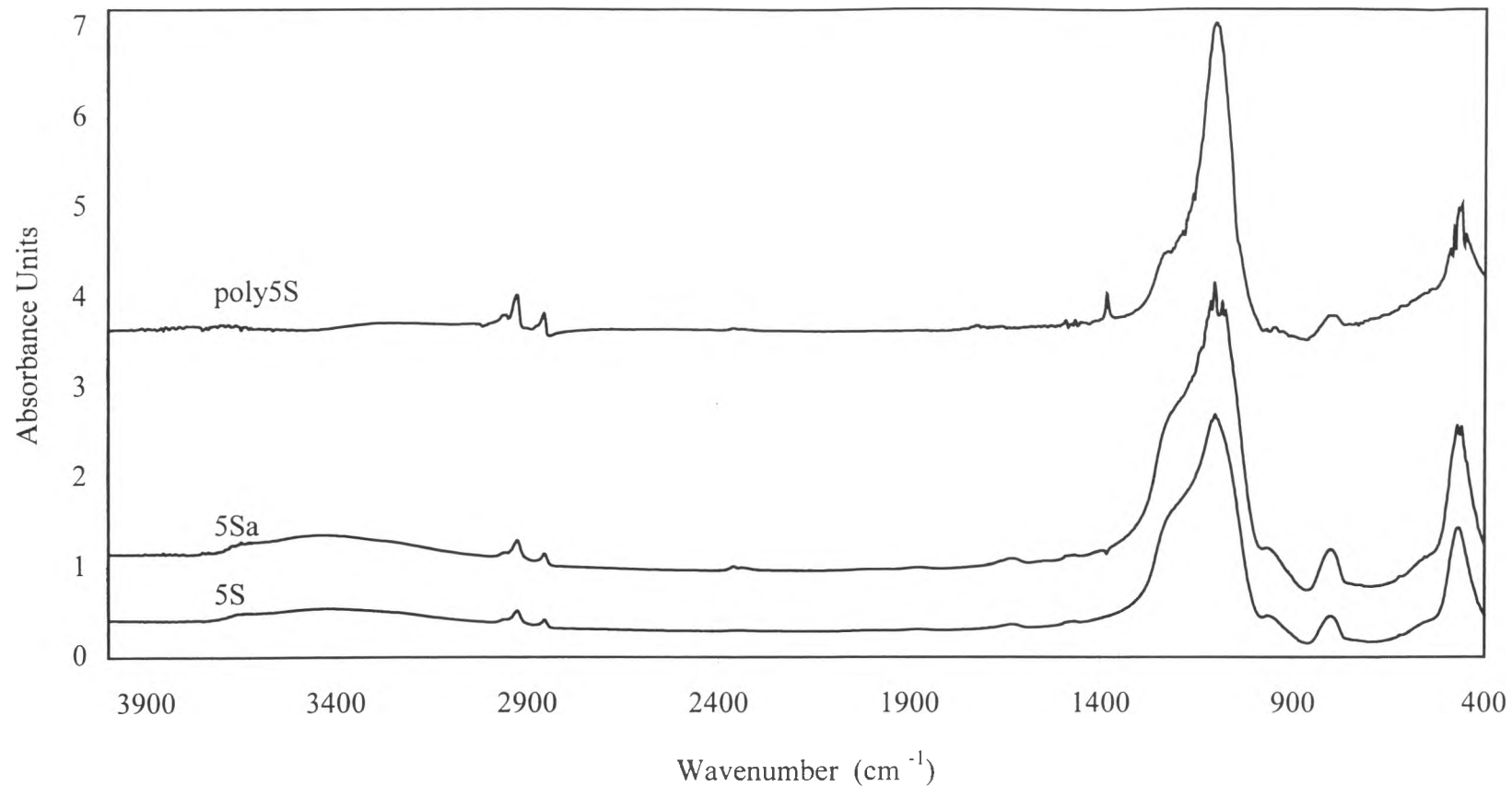


Figure 4.19 FT-IR spectra of the modified silica (5S), the modified silica after the extraction (5Sa) and the extracted material (poly5S).

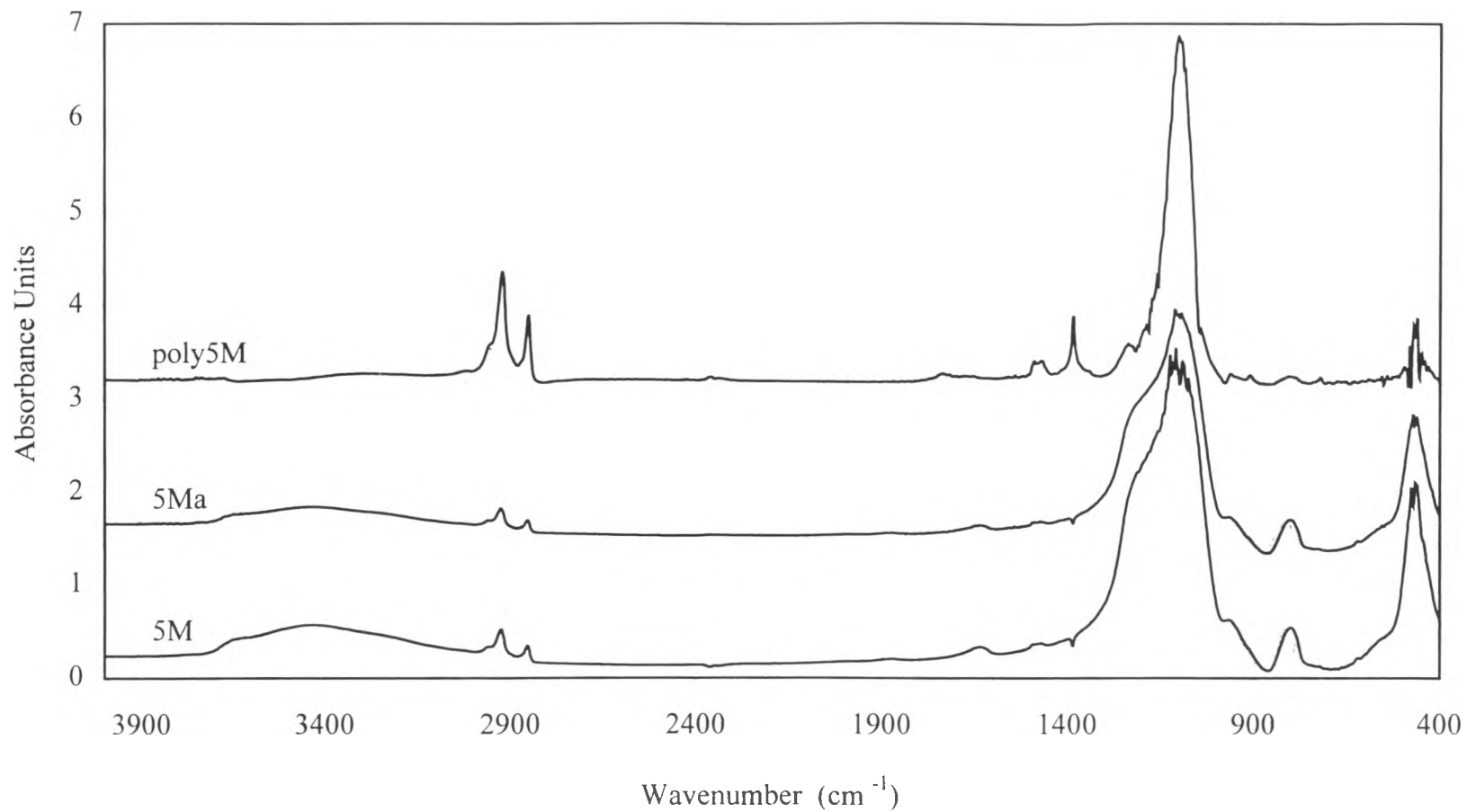


Figure 4.20 FT-IR spectra of the modified silica (5M), the modified silica after the extraction (5Ma) and the extracted material (poly5M).

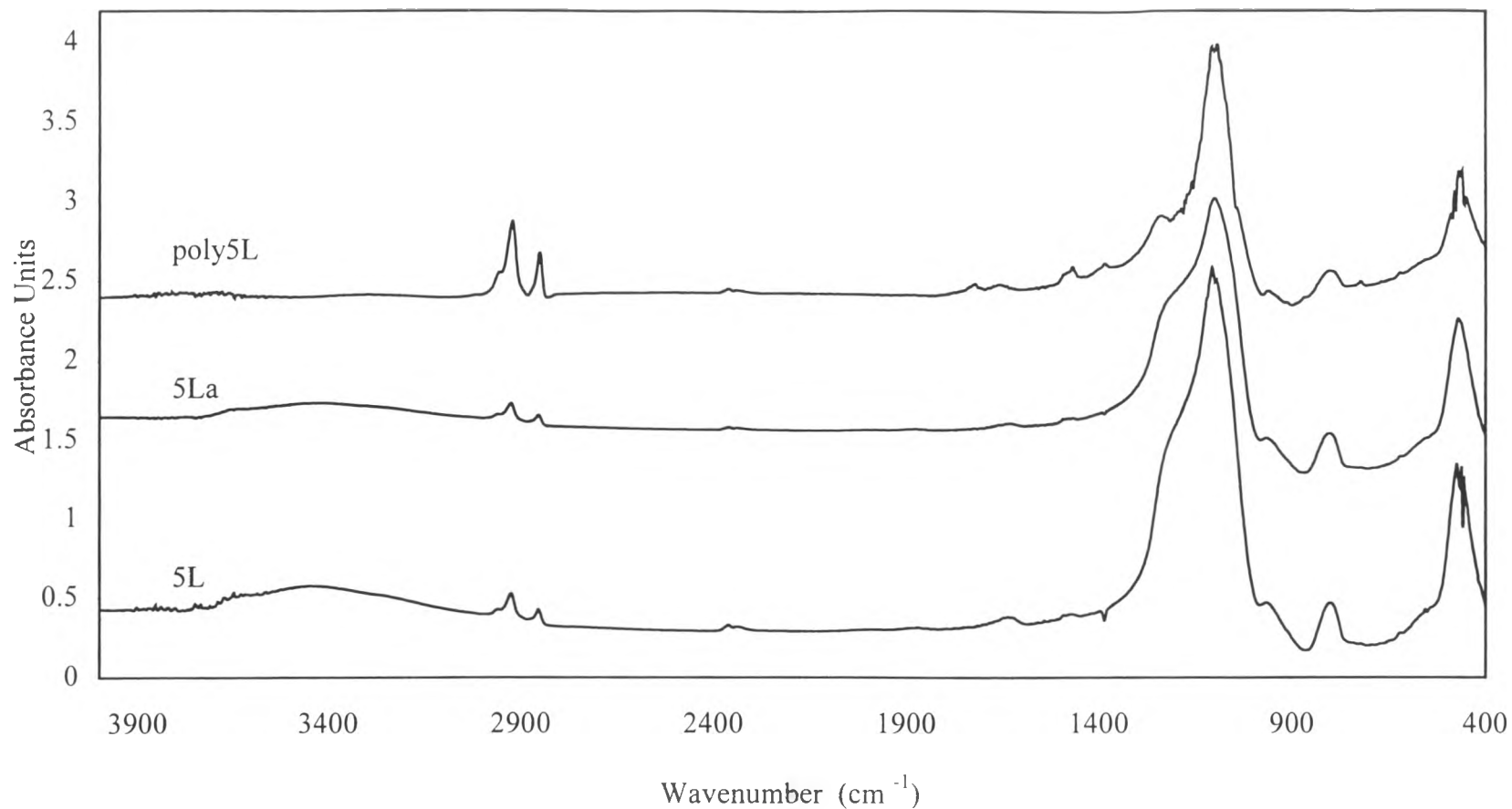


Figure 4.21 FT-IR spectra of the modified silica (5L), the modified silica after the extraction (5La) and the extracted material (poly5L).

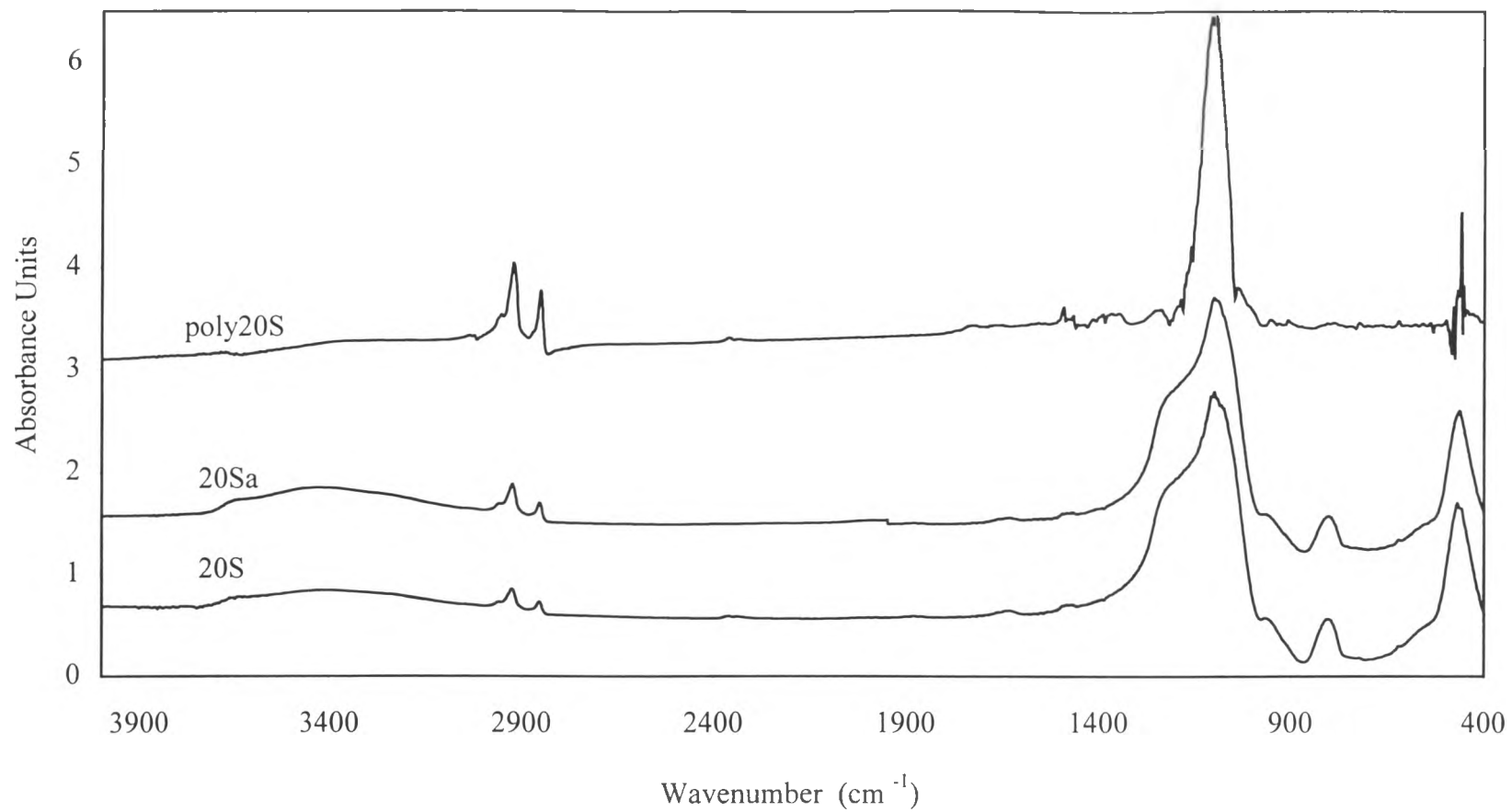


Figure 4.22 FT-IR spectra of the modified silica (20S), the modified silica after the extraction (20Sa) and the extracted material (poly20S).

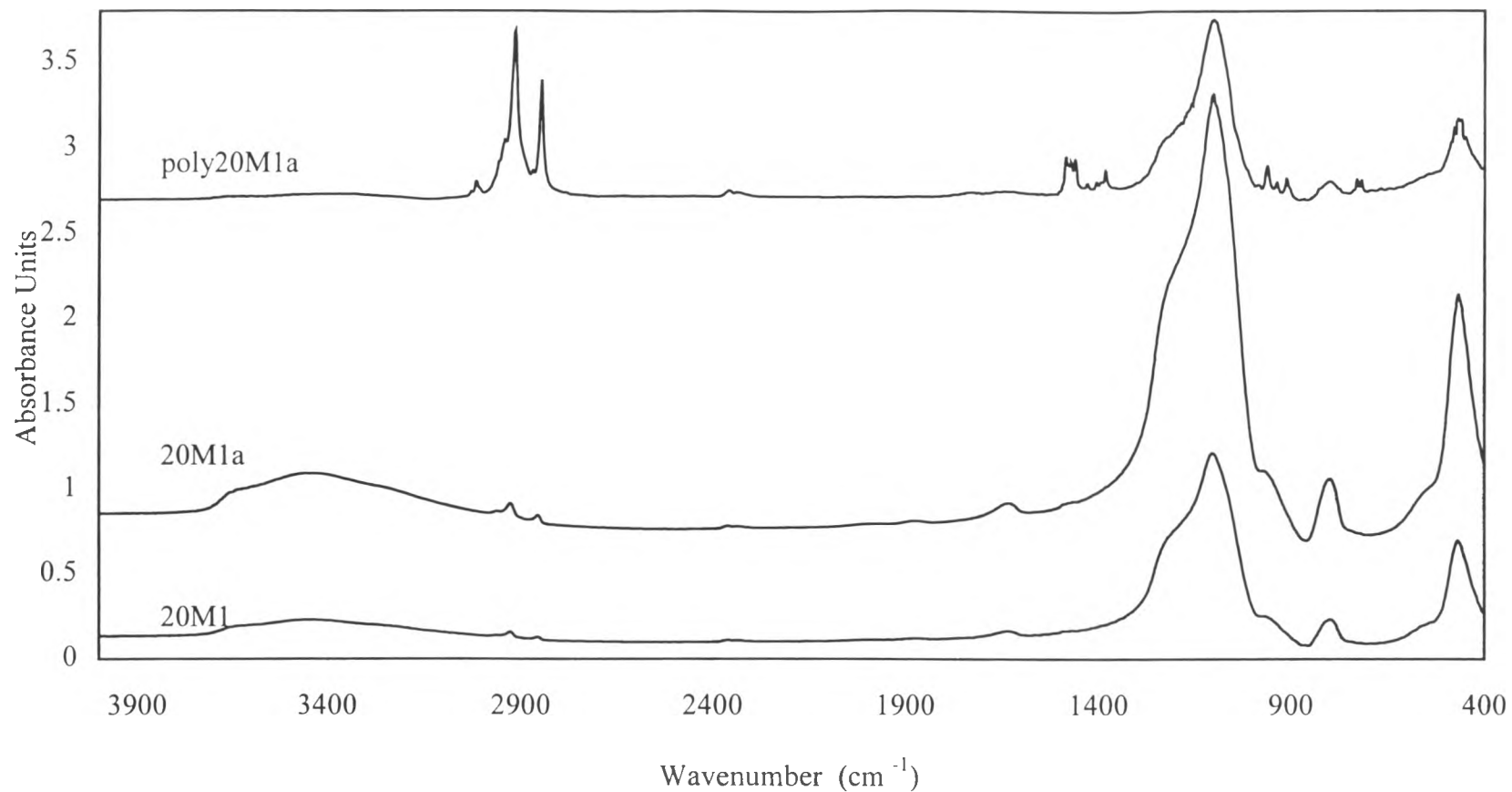


Figure 4.23 FT-IR spectra of the modified silica, (20M1), the modified silica after the extraction (20M1a) and the extracted material (poly20M1).

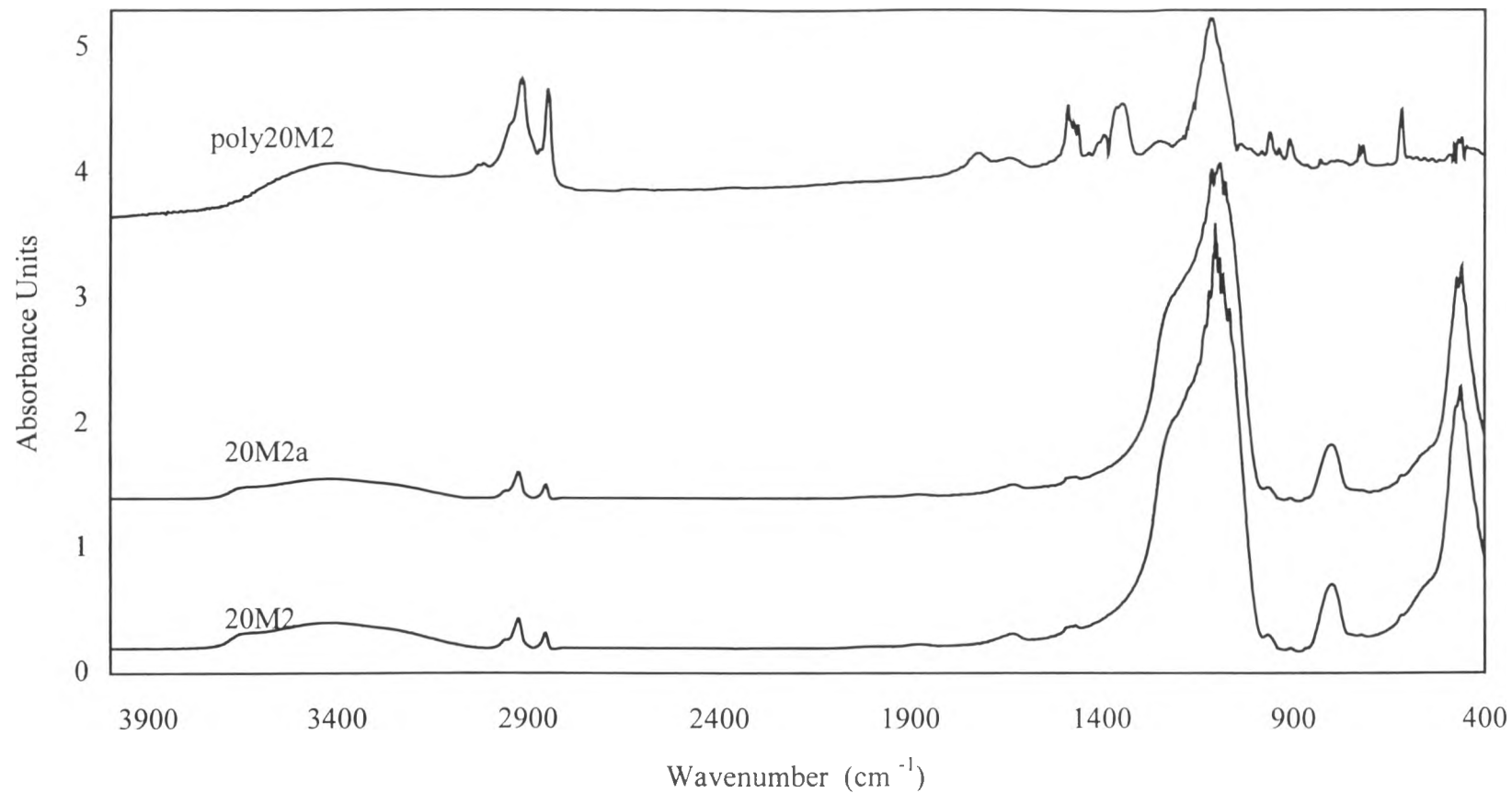


Figure 4.24 FT-IR spectra of the modified silica (20M2), the modified silica after the extraction (20M2a) and the extracted material (poly20M2).

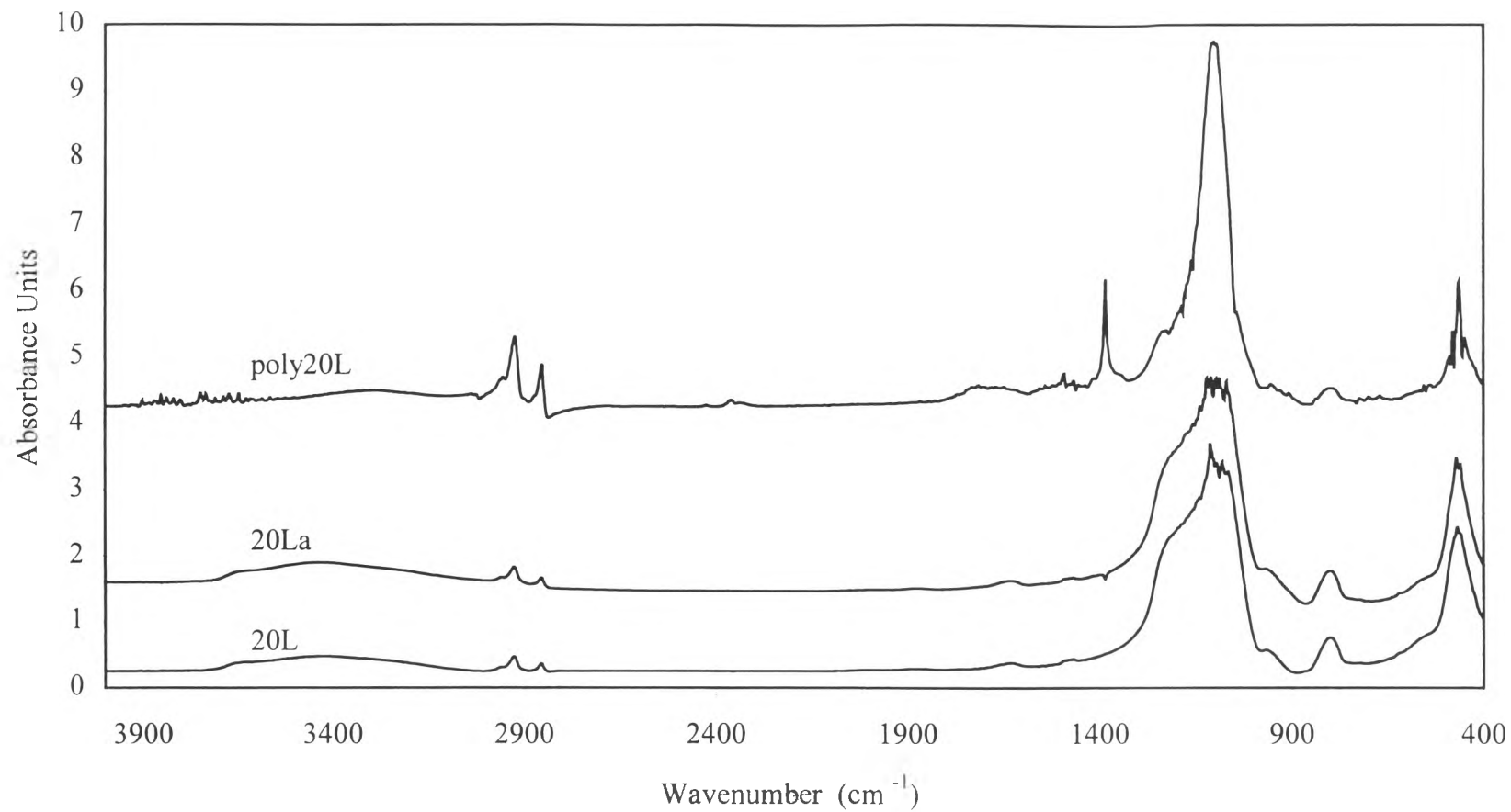


Figure 4.25 FT-IR spectra of the modified silica (20L), the modified silica after the extraction (20La) and the extracted material (poly20L).

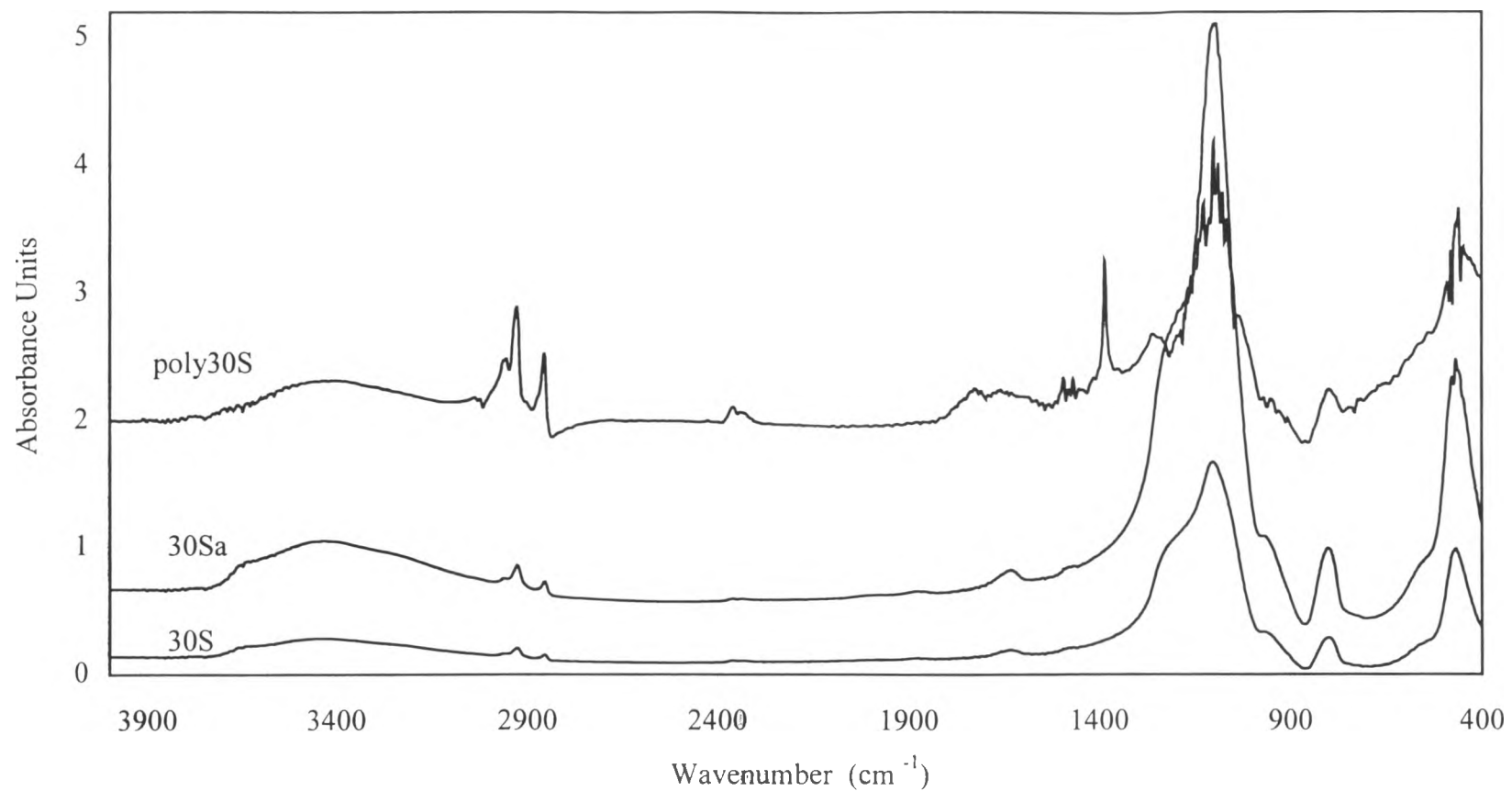


Figure 4.26 FT-IR spectra of the modified silica (30S), the modified silica after the extraction (30Sa) and the extracted material (poly30S).

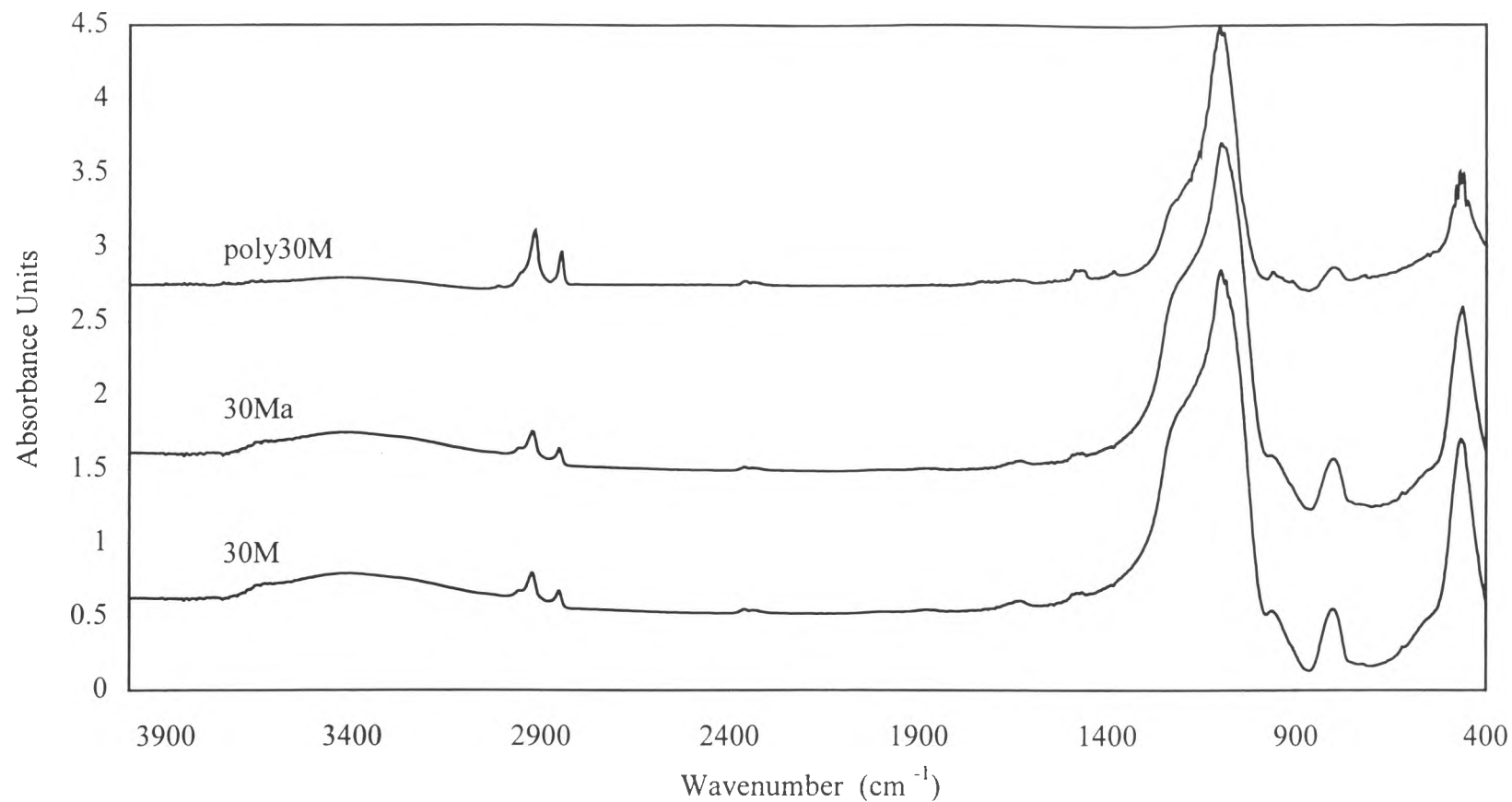


Figure 4.27 FT-IR spectra of the modified silica (30M), the modified silica after the extraction (30Ma) and the extracted material (poly30M).

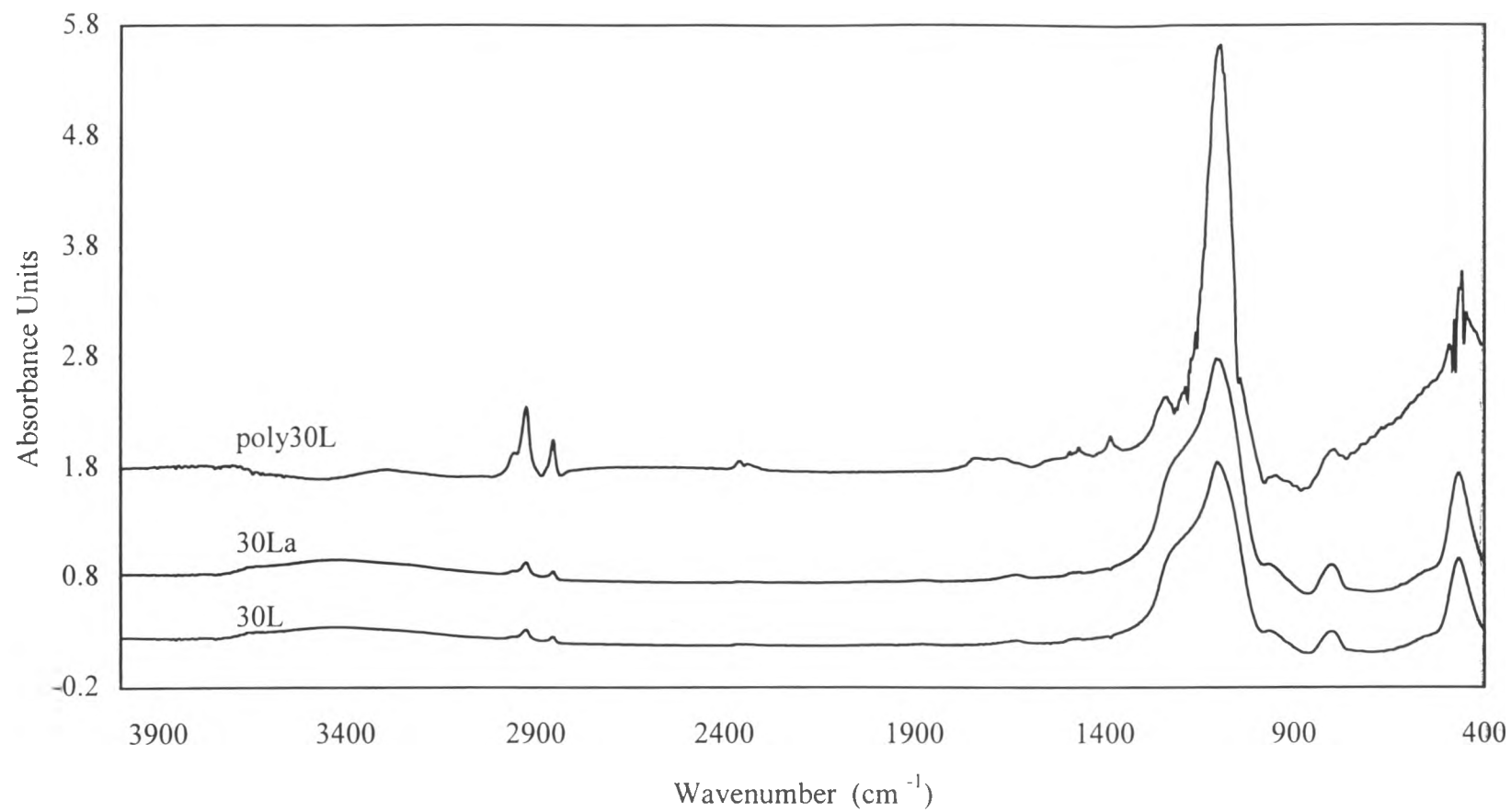


Figure 4.28 FT-IR spectra of the modified silica (30L), the modified silica after the extraction (30La) and the extracted material (poly30L).

4.3.5 Thermogravimetric Analysis (TGA) Results

All samples were examined by thermogravimetric analysis, in order to verify the existence of poly(styrene-isoprene) formed on the silica surfaces.

Figure 4.29 shows the water loss from the unmodified silica below 150°C. Thus, any weight change of the modified silicas above 150°C should be the result of the surface modification. It was found that the extraction does not affect the weight change pattern of the silica above 150°C.

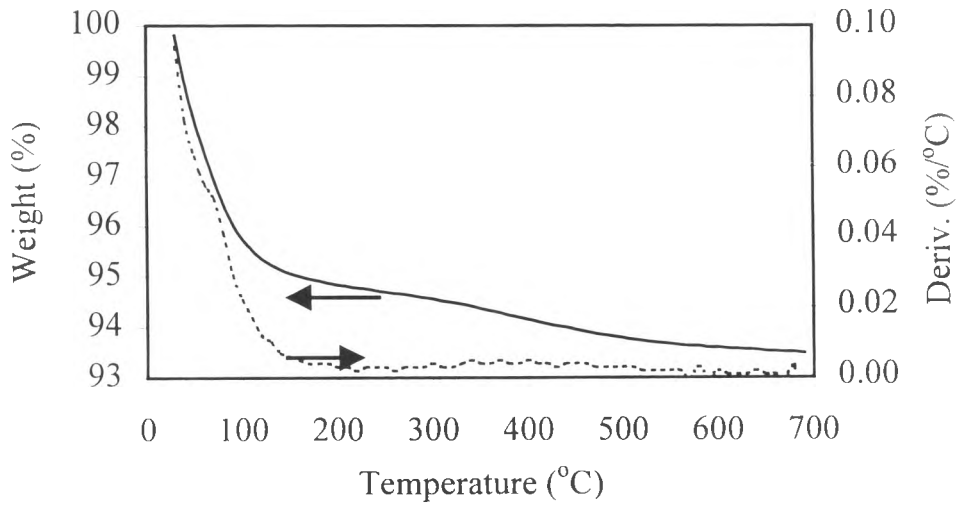
Figure 4.30 shows the decomposition of CTAB at temperatures between 200 to 300°C Figure 4.31 shows the decomposition of CTAB adsorbed onto silica, which appears to occur in two steps, the first from 170 to 300°C and the second from 300 to 450°C. The second peak of weight loss may result from the stronger bonding, chemisorption, between CTAB and silica.

To predict the decomposition temperature of poly(styrene-isoprene) of modified silica, a sample was prepared by depositing polystyrene dissolved with THF onto the silica surface. Figure 4.32 shows that the decomposition of polystyrene takes place between 350 and 480°C. The decomposition of poly(styrene-isoprene) from admicellar polymerization modified silica is shown in Figure 4.33. The graphs clearly show the decomposition of CTAB from 200 to 280°C and 300 to 450°C while that of the polymer is from 280 to 400°C.

Figures 4.34 to 4.43 show the TGA results of modified silicas before and after THF extraction. The results again showed a two-step decomposition process. The first-step is the CTAB deformation at 150 to 300°C. The second one is CTAB chemisorbed on the silica as well as poly(styrene-isoprene) decomposition at 300 to 400°C. To calculate the amount of polymer present, the amount of CTAB decomposing is calculated from the first weight drop, and this is subtracted from the weight lose at the second

peak. The amount of extracted polymer was then calculated. It was found that not all polymer can be extracted from the modified silica as confirmed by O'Haver *et al.* (1994). As shown in Table 4.1, the 5 g co-monomer loading with 60 minutes reaction time provided the highest polymer on the silica surface.

A. Unmodified silica before extraction.



B. Unmodified silica after extraction.

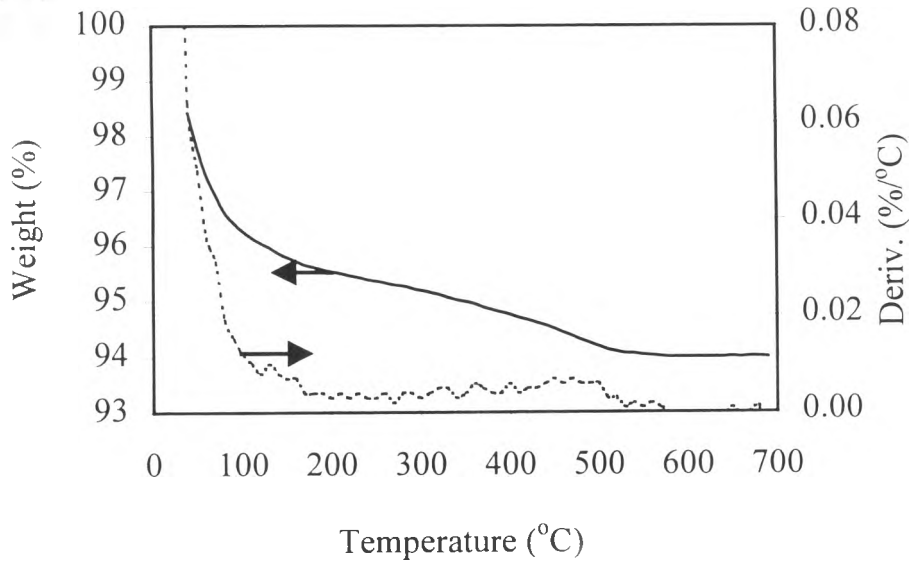


Figure 4.29 TGA results of unmodified silica Hi-Sil[®] 255.

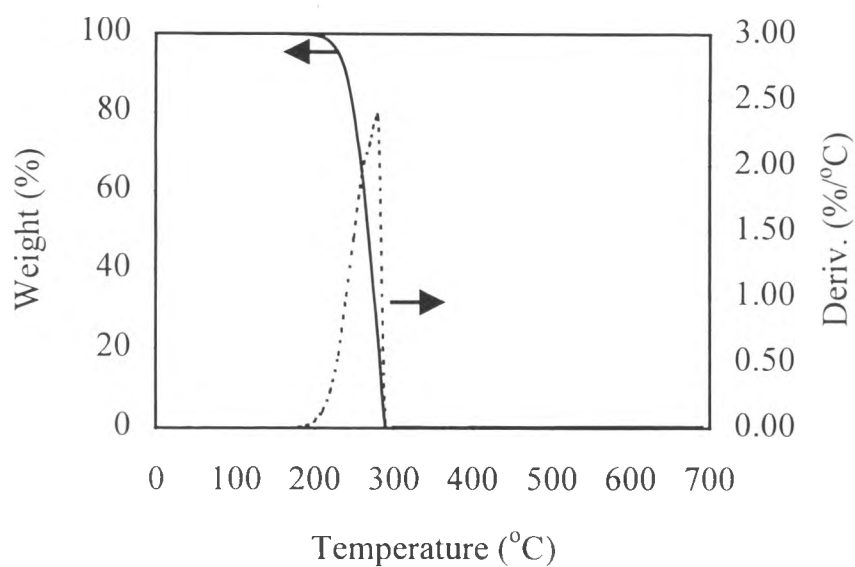


Figure 4.30 TGA results of cytrimethylammonium bromide (CTAB).

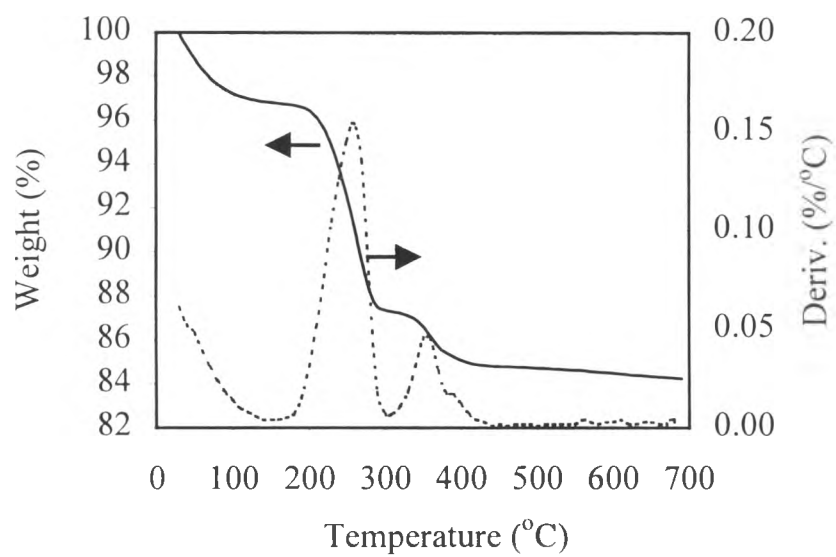


Figure 4.31 TGA results of silica Hi-Sil[®]255 adsorbed with CTAB.

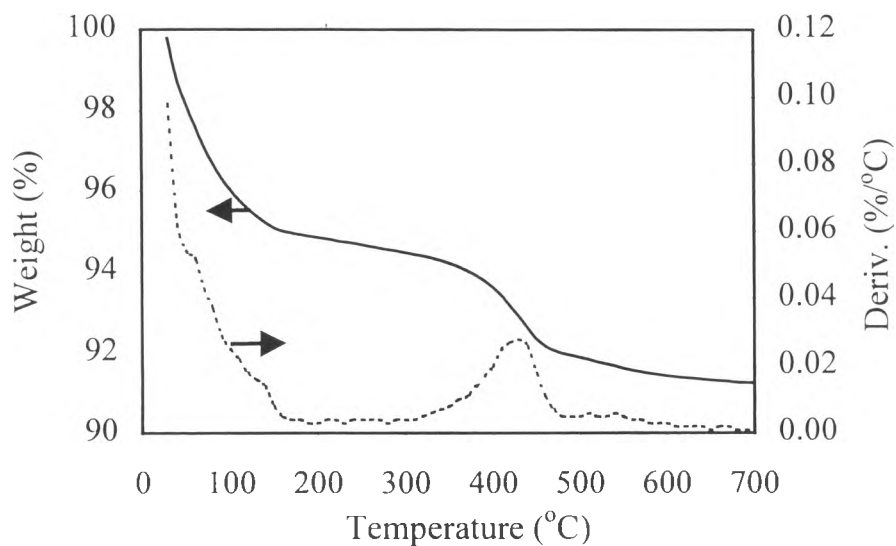


Figure 4.32 TGA results of silica Hi-Sil[®]255 adsorbed with polystyrene.

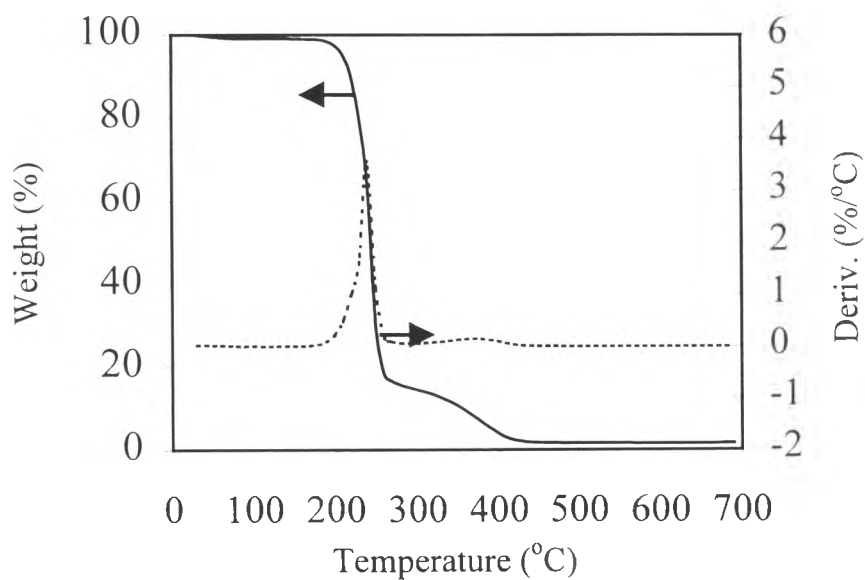
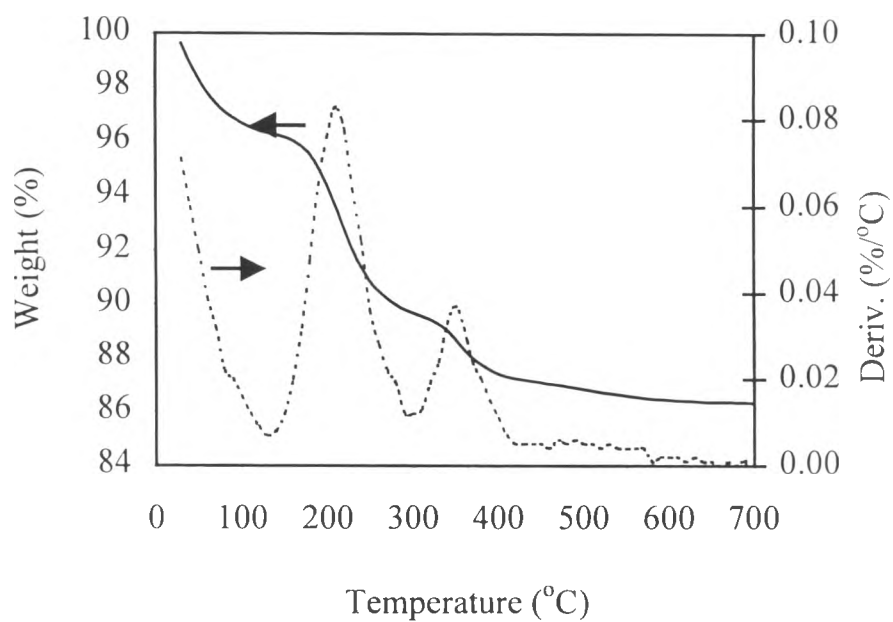


Figure 4.33 TGA results of poly(styrene-isoprene) polymerized in CTAB.

A. Modified silica before extraction.



B. Modified silica after extraction.

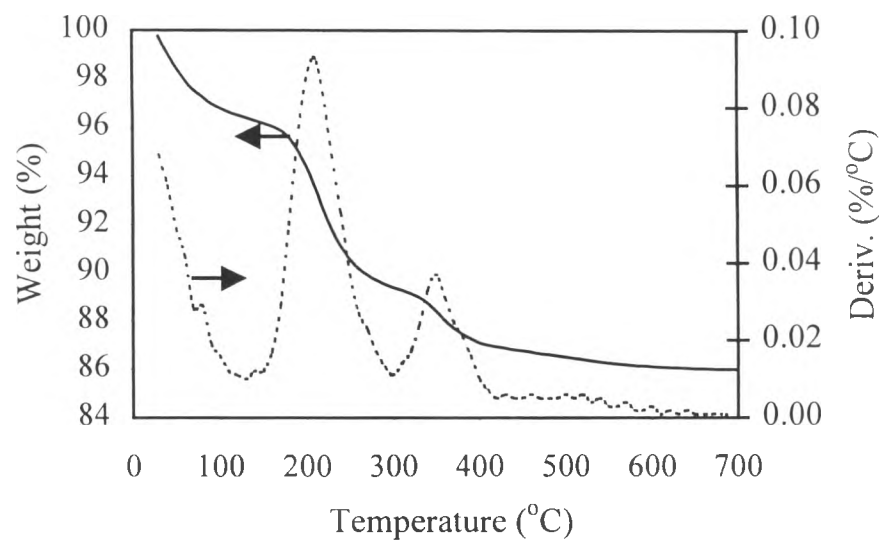
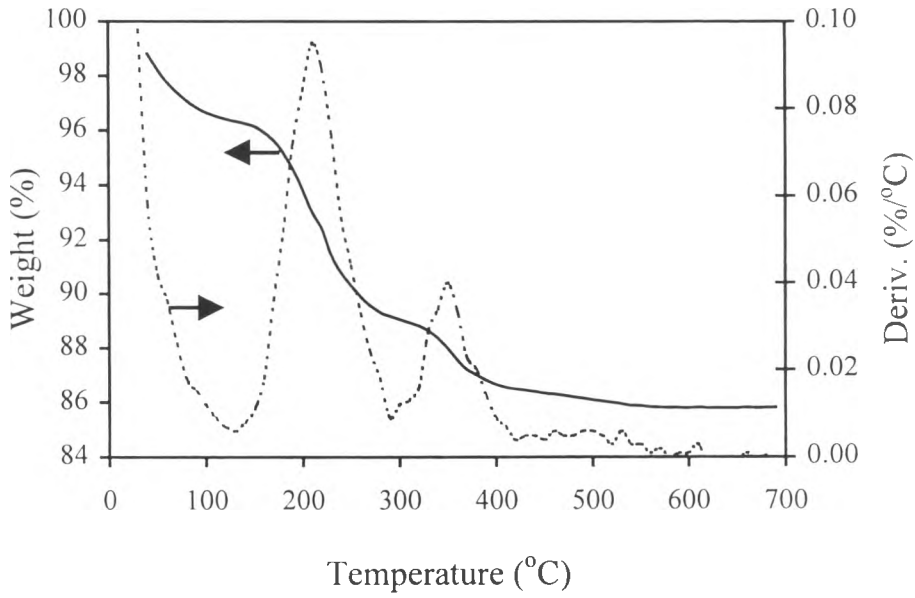


Figure 4.34 TGA results of modified silica, 5S.

A. Modified silica before extraction.



B. Modified silica after extraction.

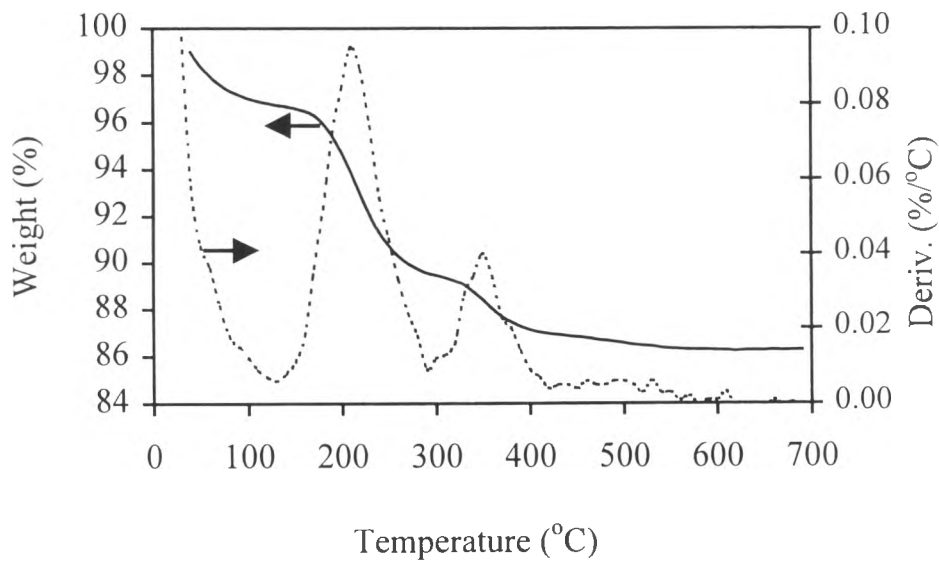
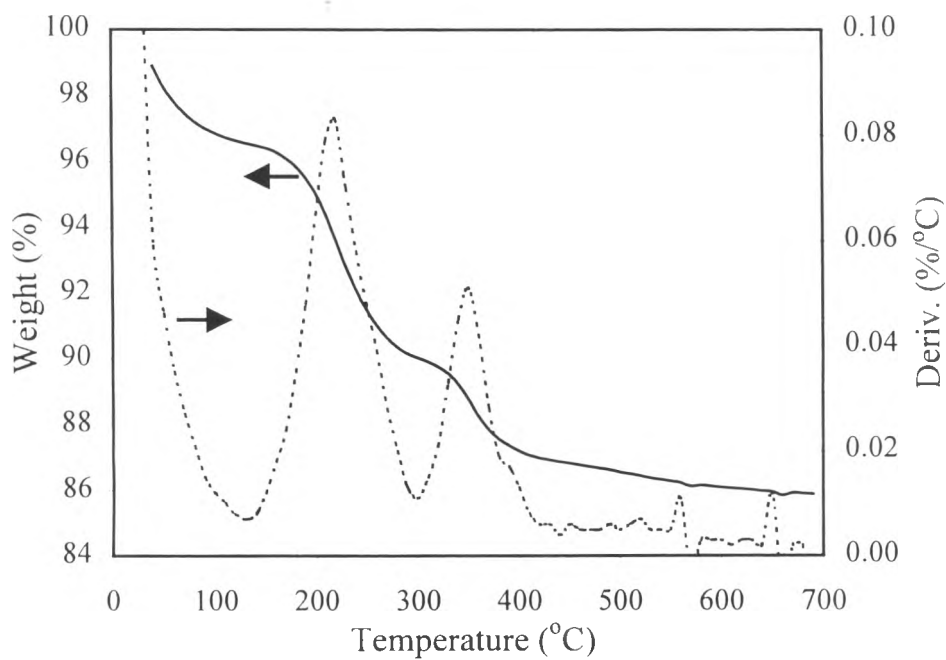
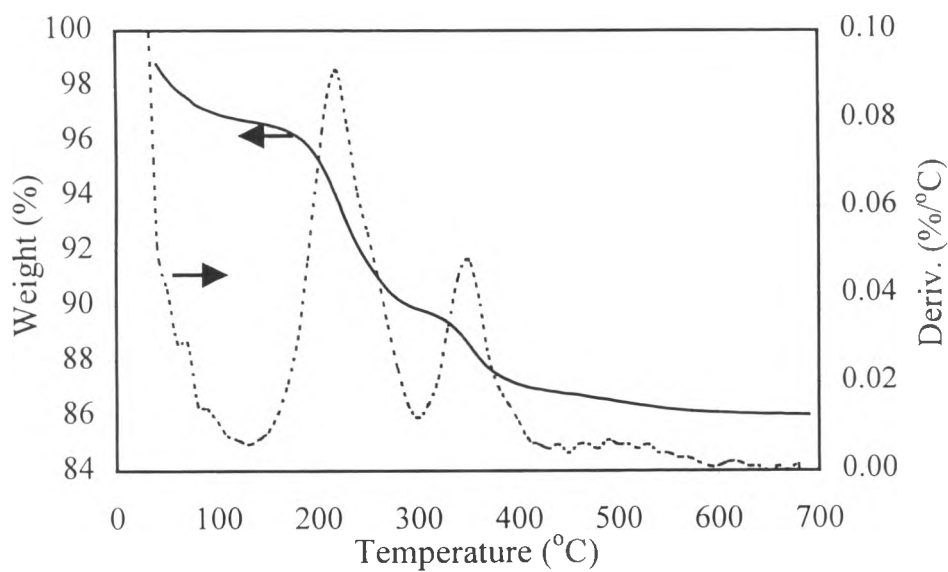


Figure 4.35 TGA results of modified silica, 5M.

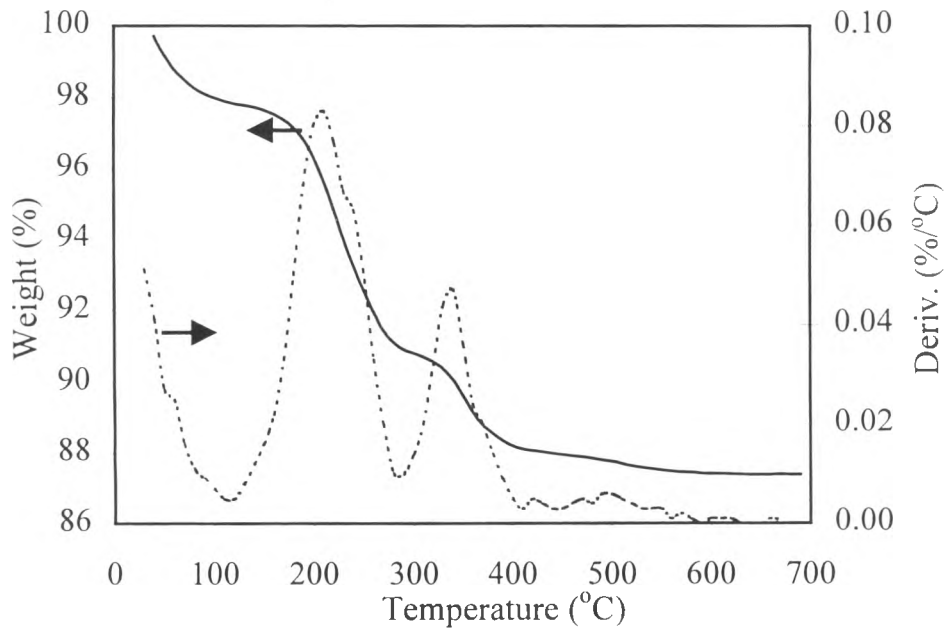
A. Modified silica before extraction.



B. Modified silica after extraction.

**Figure 4.36** TGA results of modified silica, 5L.

A. Modified silica before extraction.



B. Modified silica after extraction.

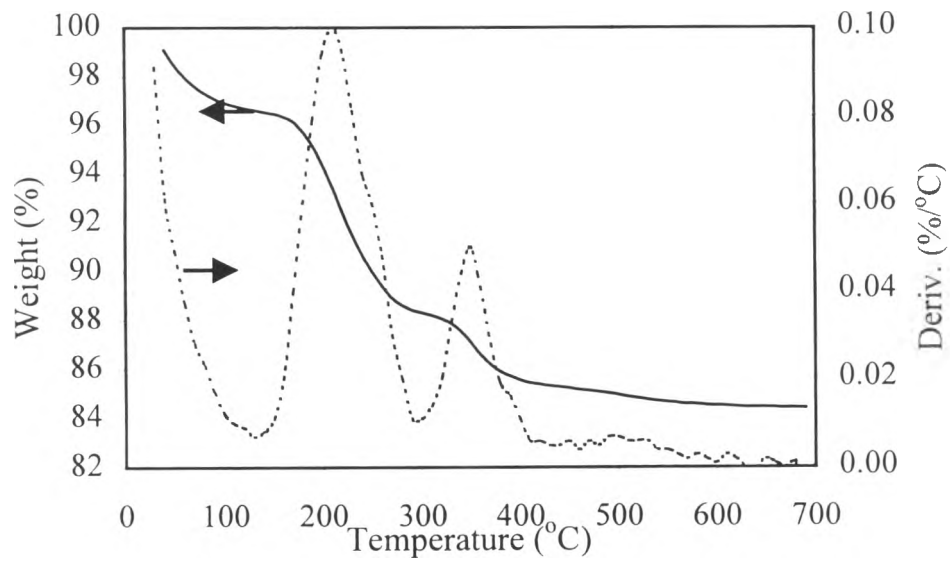
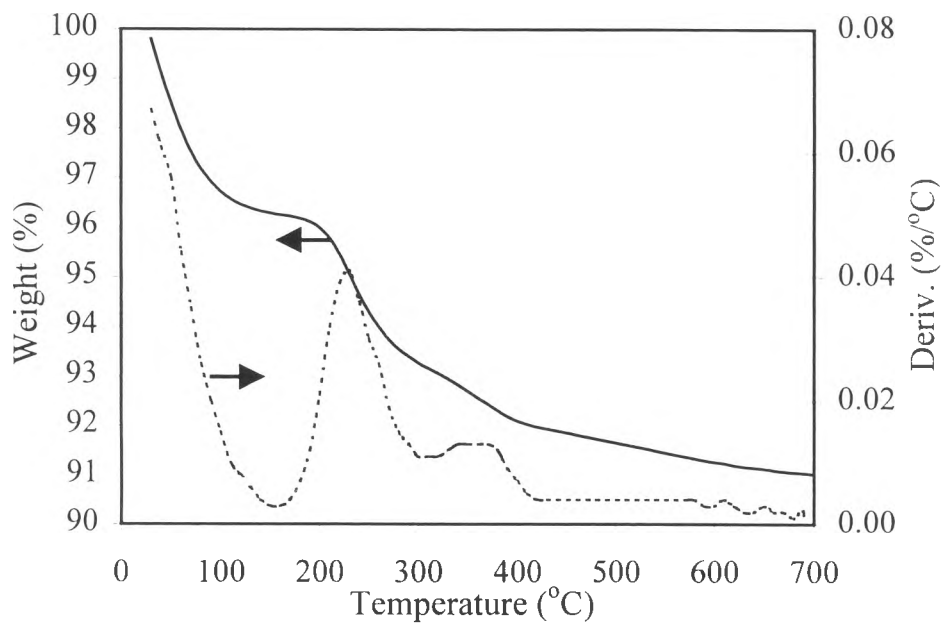


Figure 4.37 TGA results of modified silica, 20S.

A. Modified silica before extraction.



B. Modified silica after extraction.

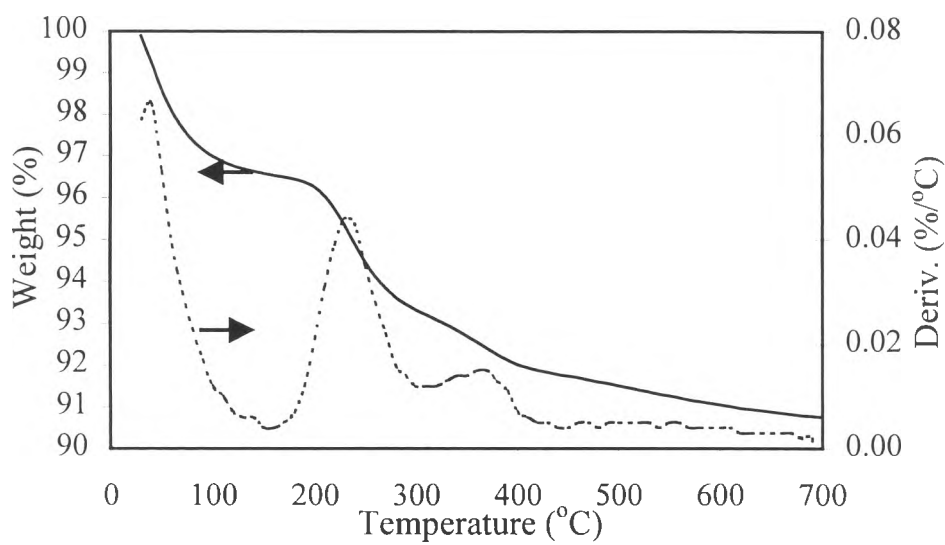
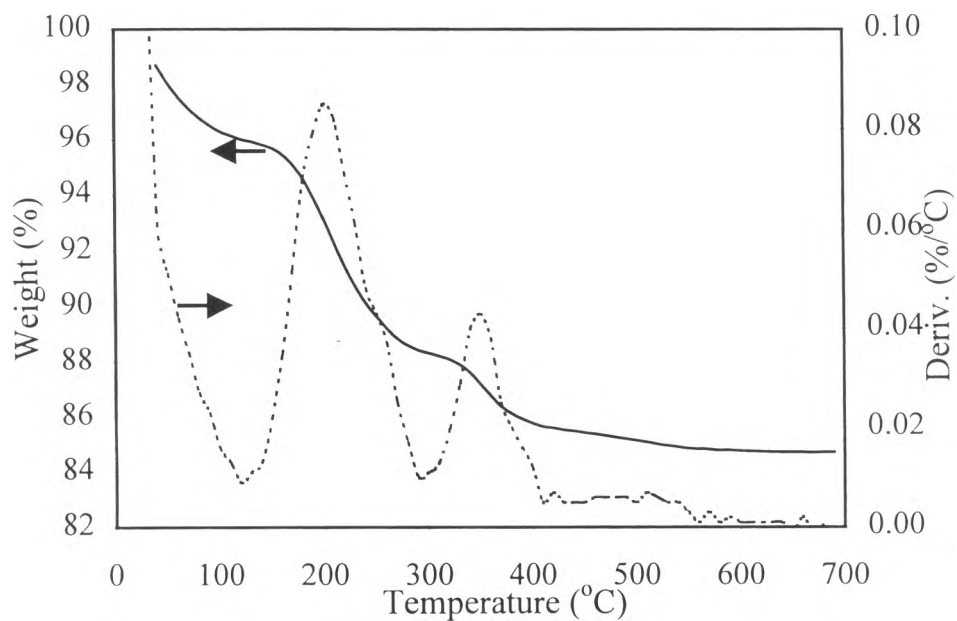


Figure 4.38 TGA results of modified silica, 20M1.

A. Modified silica before extraction.



B. Modified silica after extraction.

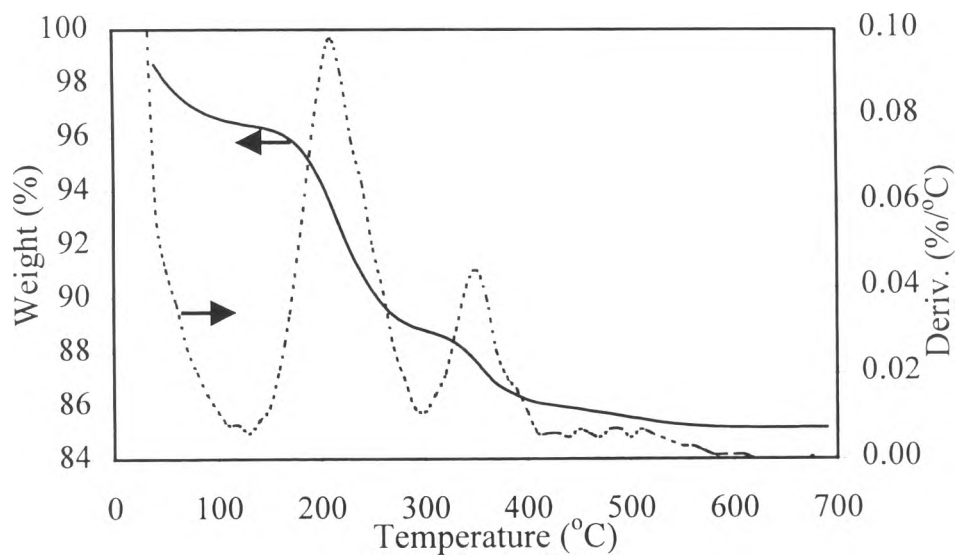
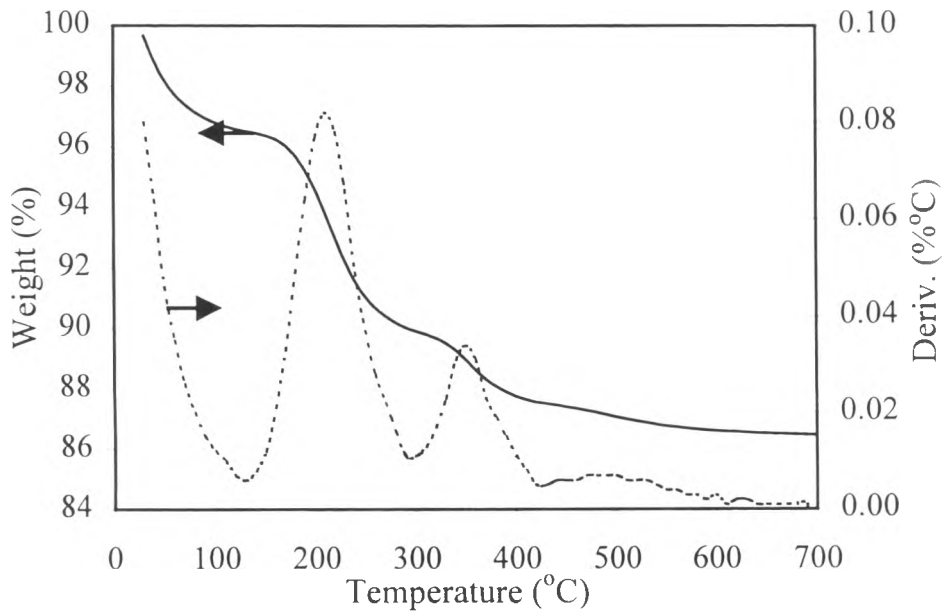


Figure 4.39 TGA results of modified silica, 20M2.

A. Modified silica before extraction.



B. Modified silica after extraction.

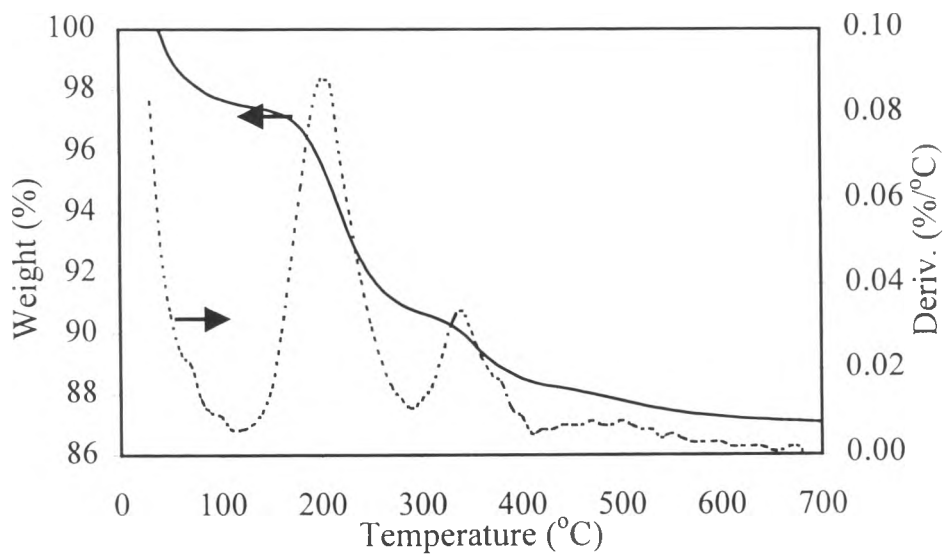
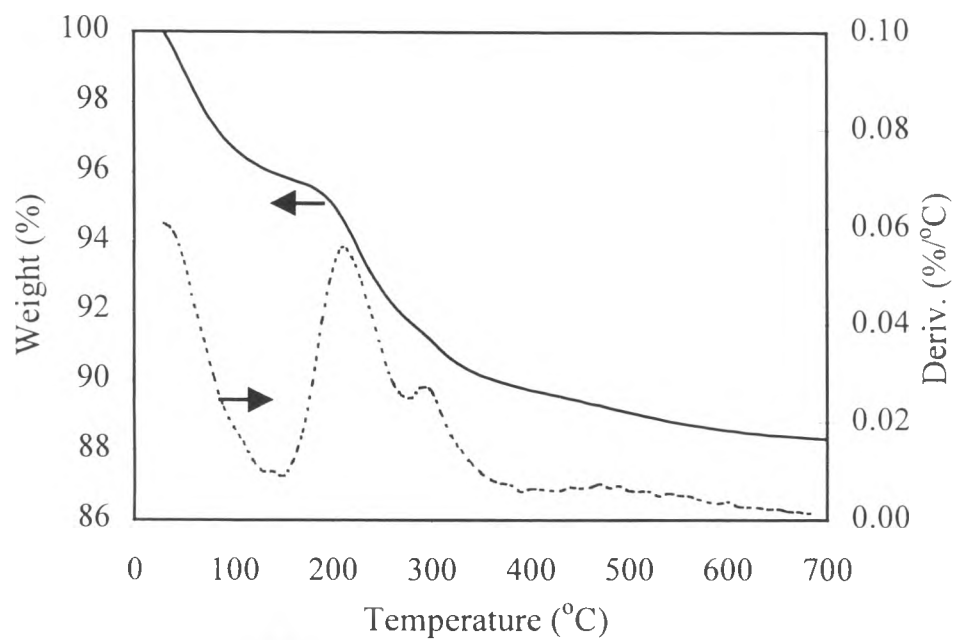


Figure 4.40 TGA results of modified silica, 20L.



A. Modified silica before extraction.



B. Modified silica after extraction.

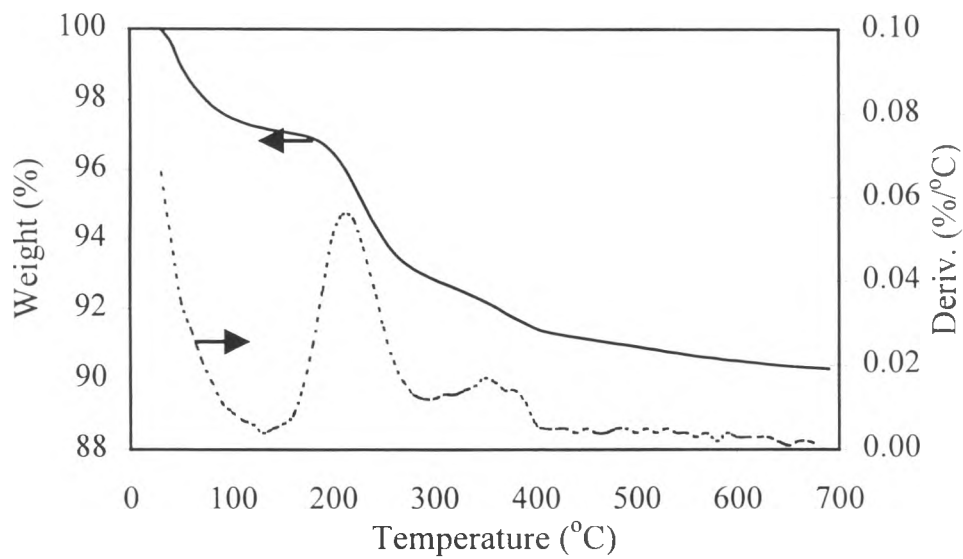
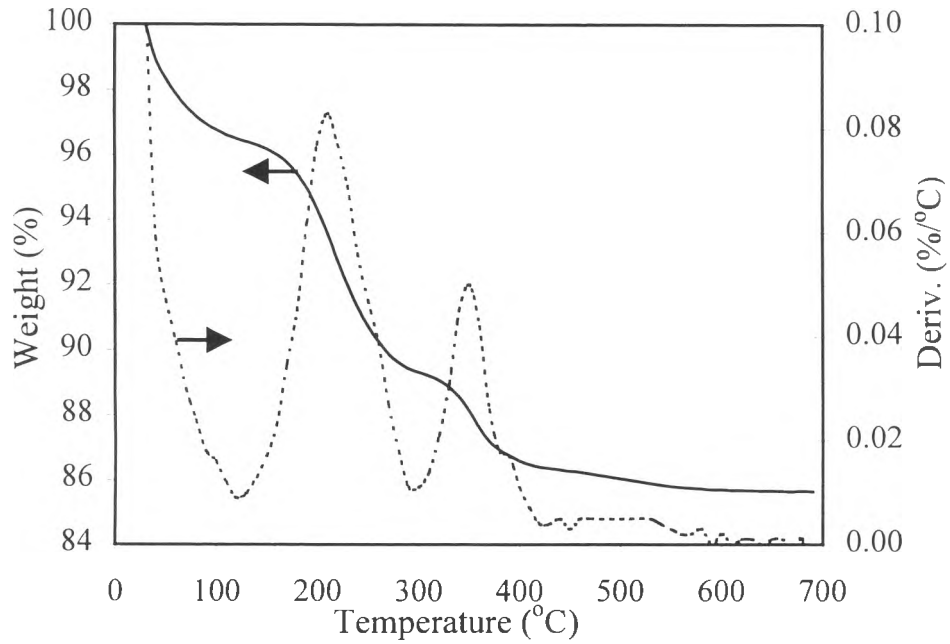


Figure 4.41 TGA results of modified silica, 30S.

A. Modified silica before extraction.



B. Modified silica after extraction.

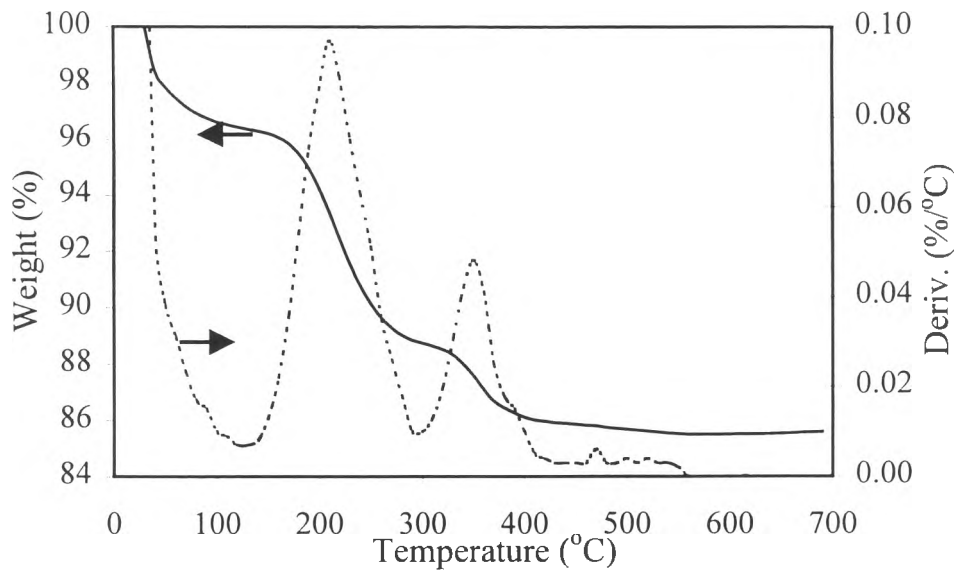
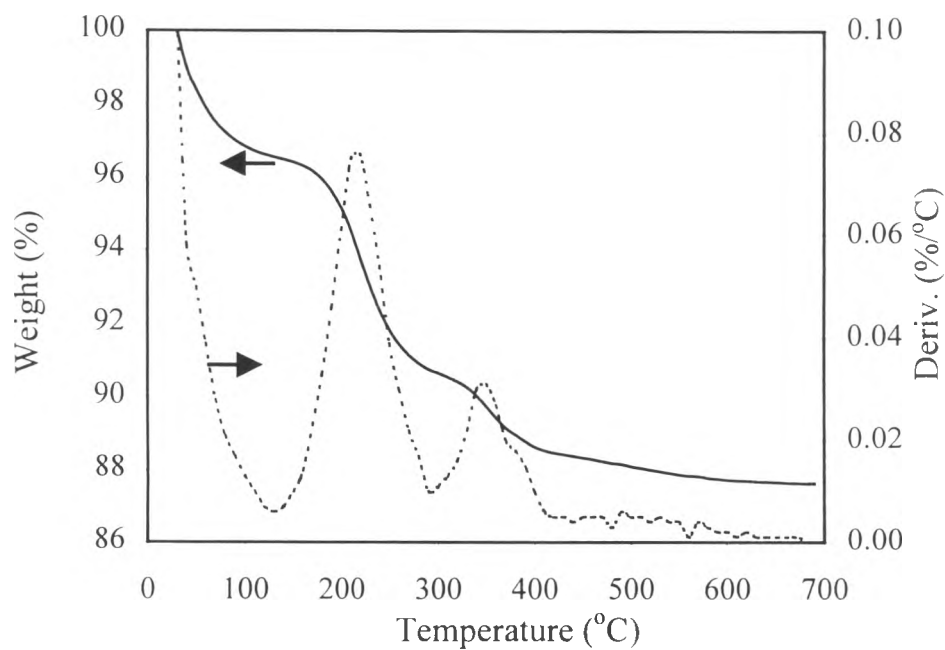


Figure 4.42 TGA results of modified silica, 30M.

A. Modified silica before extraction.



B. Modified silica after extraction.

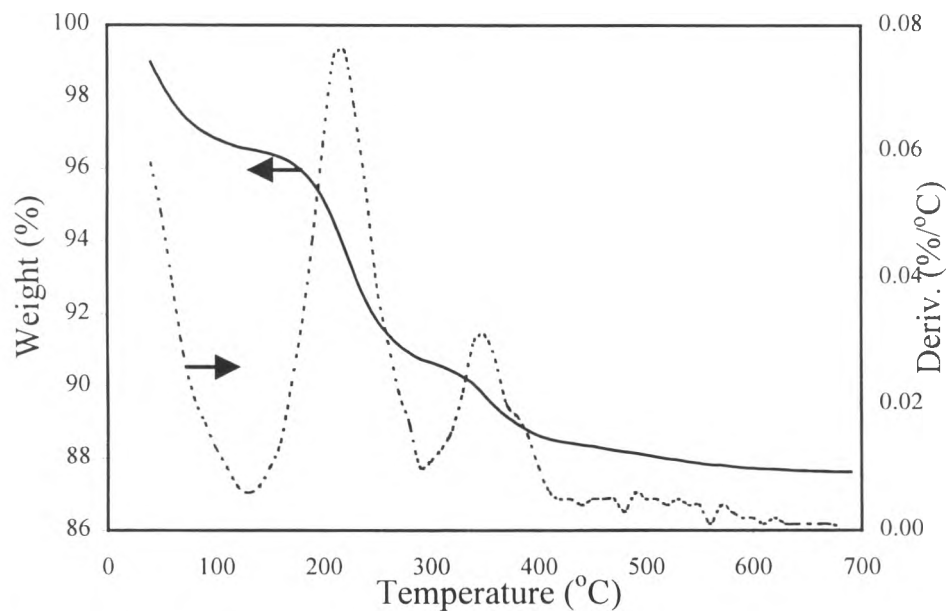


Figure 4.43 TGA results of modified silica, 30L.

Table 4.1 TGA results of modified silicas with different retention times and co-monomer loadings.

Sample		TGA (%wt. Loss)		
		Calculated Polymer		% Extracted Polymer
Monomer loading (g/kg silica)	Retention time*	Before THF Extraction	After THF Extraction	
5	S	1.220	1.013	20.74
	M	1.008	0.942	6.64
	L	1.677	1.520	15.63
20	S	1.253	1.116	13.67
	M1	0.907	0.805	10.20
	M2			
	L	1.156	1.045	11.10
30	S	0.739	0.631	10.77
	M	1.456	1.263	19.35
	L	1.201	0.961	24.00

*S = 30 min

M= 45 min

L = 60 min